Impact of track discretisation on conflict detection and resolution under ETCS with onboard train integrity monitoring

Versluis, Nina D.; Pellegrini, Paola; Quaglietta, Egidio; Goverde, Rob M.P.; Rodriguez, Joaquin

DOI
10.1016/j.jrtpm.2025.100533

Publication date
2025

Document Version
Final published version

Published in
Journal of Rail Transport Planning & Management

Citation (APA)
Versluis, N. D., Pellegrini, P., Quaglietta, E., Goverde, R. M. P., & Rodriguez, J. (2025). Impact of track discretisation on conflict detection and resolution under ETCS with onboard train integrity monitoring. *Journal of Rail Transport Planning & Management*, *35*, Article 100533. https://doi.org/10.1016/j.jrtpm.2025.100533

Journal of Rail Transport Planning & Management 35 (2025) 100533

Contents lists available at ScienceDirect

Journal of Rail Transport Planning & Management

journal homepage: www.elsevier.com/locate/jrtpm

Impact of track discretisation on conflict detection and resolution under ETCS with onboard train integrity monitoring

Nina D. Versluis [a,*], Paola Pellegrini [b], Egidio Quaglietta [a], Rob M.P. Goverde [a], Joaquin Rodriguez [b]

[a] Department of Transport and Planning, Delft University of Technology, Stevinweg 1, 2628 CN Delft, The Netherlands
[b] COSYS-ESTAS, Université Gustave Eiffel, 20 rue Élisée Reclus, 59650 Villeneuve d'Ascq, France

ARTICLE INFO

Keywords:
Railway traffic management
Train rescheduling
Railway signalling
Virtual block
Moving block

ABSTRACT

To further improve the capacity on the European railway network, next-generation distance-to-go signalling systems are being developed in the context of the European Train Control System (ETCS). This paper investigates the impact of track discretisation granularity on conflict detection and resolution for ETCS with onboard train integrity monitoring. The study enhances a previously developed model for fixed-block distance-to-go signalling by introducing a track discretisation procedure and reformulating safe train separation constraints at switches. The assessment is performed on a junction and a corridor case study, using track discretisations with maximum section lengths from 50 to 800 m. Though finer discretisations potentially improve the model objective, computation times quickly increase. While the results show minimum effects of the track discretisation on the conflict detection and resolution, they suggest that maximum section lengths of 200 or 400 m may offer a good balance between solution quality and computational complexity, depending on the track layout and traffic density. Generally, reliable rescheduling decisions can already be obtained with a 800-m discretisation.

1. Introduction

On the railway network, safe operations are ensured through railway signalling. On the one hand, trains are separated by providing and supervising a movement authority (MA) and corresponding dynamic speed profile, i.e., the permission to move to a specific location under distance and speed monitoring, to the trains. On the other hand, train movements are protected by setting and locking train routes over movable track elements such as switches. Train separation and route protection characteristics vary depending on the implemented signalling system.

In Europe, railway signalling systems are developed in the context of the European Train Control System (ETCS) within the European Railway Traffic Management System (ERTMS) specifications with interoperability throughout Europe as overall objective. The current state-of-practice is ETCS Level 2 with trackside train detection (TTD), which is implemented on freight and passenger railways throughout the world (European Rail Supply Industry Association, 2022). ETCS Level 2 with TTD is a radio-based fixed-block distance-to-go signalling system which relies on TTD for train position and integrity monitoring. In fixed-block signalling systems, the track is partitioned into blocks (or sections) of fixed lengths which can be occupied by at most one train at a time. In legacy systems, block entries are protected by trackside multi-aspect signals which indicate whether an approaching train can

* Corresponding author.
E-mail addresses: n.d.versluis@tudelft.nl (N.D. Versluis), paola.pellegrini@univ-eiffel.fr (P. Pellegrini), e.quaglietta@tudelft.nl (E. Quaglietta), r.m.p.goverde@tudelft.nl (R.M.P. Goverde), joaquin.rodriguez@univ-eiffel.fr (J. Rodriguez).

https://doi.org/10.1016/j.jrtpm.2025.100533
Received 20 December 2024; Received in revised form 23 April 2025; Accepted 19 June 2025
Available online 8 July 2025

proceed, needs to start braking or is required to stop. Additionally, distant signals can be used to indicate the approach of a restrictive main signal in two-aspect signalling. Distance-to-go signalling systems, instead, feature radio-based cab signalling and continuous braking curve supervision from the train front position to the section exit corresponding to the end of MA. With this, brake indications can be given to a train at any point on the track. As a consequence, train separation distances become speed-dependent due to the approach distance to the first occupied section being based on the train's absolute braking distance.

In the next-generation distance-to-go signalling systems ETCS Level 2 Virtual Block (VB) and ETCS Level 2 Moving Block (MB), TTD is replaced by onboard train position and train integrity monitoring (TIM). These systems are collectively referred to as ETCS Level 2 with onboard TIM, which was known as ETCS Level 3 until 2023. ETCS Level 2 VB is still a fixed-block system, but the block boundaries are defined virtually instead of through trackside devices. In ETCS Level 2 MB, the track partitioning is eliminated such that the MA can be given up to a safety margin behind the train in front. Depending on the section lengths within the track partitioning, VB can be considered as an approximation of MB (Versluis et al., 2024b; Furness et al., 2017). In addition, the railway industry is currently developing ETCS Hybrid Train Detection (HTD), previously known as ETCS Hybrid Level 3 (EEIG ERTMS Users Group, 2024). That is, ETCS with limited TTD and virtual subsections, such that the MA of a train following a train not equipped with TIM will be based on TTD sections, while it will be based on the virtual subsections when it follows a train with onboard TIM.

Fig. 1 illustrates the minimum train separation in fixed-block distance-to-go signalling with a coarse track partitioning, e.g., ETCS Level 2 with TTD, and with a fine track partitioning, e.g., ETCS Level 2 VB. A comparison of the two demonstrates the effect of section length in fixed-block distance-to-go systems. Shorter sections lead to shorter train separation distances, which means more efficient operations, e.g., in terms of capacity.

In terms of train separation distances, the conventional signalling systems relate to ETCS Level 2 with TTD and ETCS Level 2 VB as follows. In legacy fixed-block systems, train separation is determined by the fixed block design and the braking capabilities of the train, which together define the admissible speed and safe stopping distances. As a result, separation distances are generally larger than those in ETCS Level 2 with TTD. Under ETCS HTD, the minimum separation depends on whether the preceding train is equipped with onboard TIM. If so, the separation distance is as under ETCS Level 2 VB. If not, the separation distance is as under ETCS Level 2 with TTD. Under ETCS Level 2 MB, the train separation is the shorter than under ETCS Level VB due to the independence of track discretisation.

In case of disturbed railway operations, railway traffic management is responsible for the efficient use of the available capacity. The problem of taking effective rescheduling measures in order to minimise train delays in case of disturbances can be mathematically described in conflict detection and resolution models. There are, however, very limited conflict detection and resolution models for next-generation distance-to-go signalling systems, e.g., ETCS Level 2 with onboard TIM (Versluis et al., 2024b).

In previous work, we have addressed this gap by proposing an approach to enhance existing conflict detection and resolution models to describe fixed-block distance-to-go railway operations (Versluis et al., 2024a). The incorporation of the enhancements into the state-of-the-art rescheduling model RECIFE-MILP (Pellegrini et al., 2015) resulted in a verified conflict detection and resolution model for ETCS Level 2 with TTD. A comparison of the enhanced with the original model indicated that other rescheduling decisions can be proposed due to the exploitation of distance-to-go operations to minimise train delay.

In this paper, we continue to address conflict detection and resolution for distance-to-go signalling. Building upon our previous work, we now shift the focus towards ETCS Level 2 with onboard TIM, specifically ETCS Level 2 VB. By considering ETCS Level 2 with onboard TIM parameters as input for the enhanced RECIFE-MILP, we obtain a conflict detection and resolution model for next-generation fixed-block distance-to-go signalling. Additionally, we reformulate the train separation constraints in the bottleneck areas around switches to decrease their criticality in operations. The model describes ETCS Level 2 VB, but can also serve as an

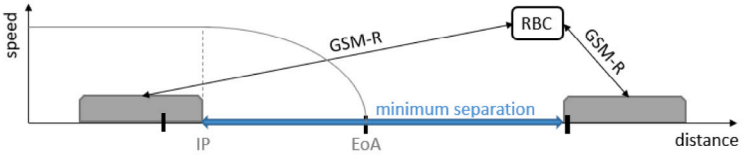

(a) Coarse track discretisation granularity, corresponding to ETCS Level 2 with TTD.

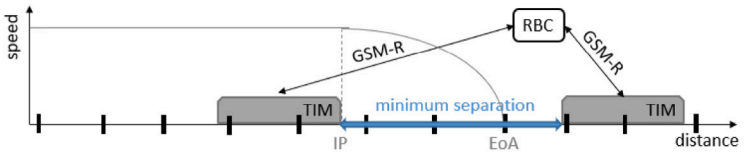

(b) Fine track discretisation granularity, corresponding to ETCS Level 2 VB.

Fig. 1. Schematic layout of the minimum separation between two trains in a speed-distance diagram under fixed-block distance-to-go signalling systems with different track discretisation granularity. EoA stands for end of movement authority and IP for the indication point of the braking curve to the EoA.

approximation of ETCS Level 2 MB. For both, the granularity of the track discretisation is a crucial modelling aspect. While the impact of track discretisation on railway capacity is well addressed in the literature, e.g., Cuppi et al. (2021), Ranjbar et al. (2022) and Knutsen et al. (2024), its effect on conflict detection and resolution has only been scarcely, if at all, investigated. This work aims to fill this gap by assessing how the track discretisation granularity affects the conflict detection and resolution model for ETCS Level 2 with onboard TIM. Specifically, we focus on the effects on rescheduling decisions, complemented by an analysis of the trade-off between solution quality and computation time.

With this, the paper's main contributions are:

- A reformulation of train separation constraints for switches based on minimum switch blocking times.
- A conflict detection and resolution model for ETCS with onboard train integrity monitoring.
- A sensitivity analysis of the conflict detection and resolution model for ETCS with onboard train integrity monitoring on track discretisation granularity.

The paper is organised as follows. In Section 2, related literature is reviewed. Section 3 introduces the approaches related to the ETCS signalling parameters, the track (re)discretisation and the reformulation of the switch blocking times. In Section 4, the computational setup and experimental results are presented and discussed. The paper is finalised with concluding remarks in Section 5.

2. Literature review

To the best of our knowledge, there is no available literature on the impact of track discretisation on conflict detection and resolution under ETCS Level 2 (or other next-generation distance-to-go signalling systems). Therefore, we divide our literature review into the following two subtopics. We address conflict detection and resolution under next-generation signalling in Section 2.1 and track discretisation in railway signalling in Section 2.2.

2.1. Towards conflict detection and resolution under ETCS level 2

Existing conflict detection and resolution models mostly refer to conventional fixed-block multi-aspect signalling systems (Versluis et al., 2024b). Two state-of-the-art models are ROMA (D'Ariano, 2008) and RECIFE-MILP (Pellegrini et al., 2015). They represent two main categories of conflict detection and resolutions models: alternative graph-based, e.g., Mazzarello and Ottiviani (2007), Corman et al. (2009) and Janssens (2022), and MILP-based models, e.g., Törnquist and Persson (2007), Pellegrini et al. (2014) and Luan et al. (2018), respectively. Actually, all MILP-based models mentioned so far are disjunctive MILP models. Another class of MILP-based models are time-indexed models, as proposed by, e.g., Lusby et al. (2013), Reynolds et al. (2020) and Bettinelli et al. (2017). Some other modelling approaches applied to conflict detection and resolution are constraint programming (Rodriguez, 2007; Marlière et al., 2023) and model predictive control (Caimi et al., 2012; Pochet et al., 2016).

The different approaches each have their own strengths and limitations in terms of, e.g., inclusion of speed, stability for rerouting, computational performance and flexibility in objective function (Versluis et al., 2024b). For example, classic alternative graph models can only feature graph-based objectives, typically the minimisation of the maximum secondary train delay as objective function, while MILP models can feature any objective as long as it can be represented by a linear function. Moreover, MILP models are more flexible in terms of rerouting. Disjunctive MILP models, however, rely on the general big-M method, resulting in a relatively weak linearisation which makes them hard to solve to optimality. The other MILP-based approach of time-indexed models is an alternative in that aspect. The time-indexed model formulation has, however, the drawback of a large model size due to the explicit need of time-space resources.

Another way to counter the limitations of big-M formulations is by decomposition of the conflict detection and resolution problem, e.g., Lamorgese and Mannino (2015), Yi et al. (2023) and Lippes (2024). Lamorgese and Mannino (2015) consider an exact macro/micro decomposition methods inspired by Benders decomposition (Benders, 1962). They propose an iterative approach between the overall problem which is solved at a macroscopic level and the subproblems which are searching feasible train routes through stations. Yi et al. (2023) also consider a macroscopic and a microscopic level of the problem. At the microscopic level, for each control area separately, rescheduling decisions are proposed by the RECIFE-MILP model. At the macroscopic level, coordination of the local decisions is performed by a time-indexed MILP model. This iterative coordination framework is independent from the approach used for the rescheduling at the microscopic level. Lippes (2024) proposes an iterative distributed approach to describe moving-block conflict detection and resolution. The model used for the conflict resolution in subareas is based on the disjunctive MILP formulation of Törnquist and Persson (2007). Lippes (2024) solves the subproblems sequentially with coordination intervention in case of dependencies. The works show significant improvements in computational performance compared to centralised approaches.

The sparse literature on conflict detection and resolution models for ETCS Level 2 or, more general, distance-to-go signalling includes the work of Pochet et al. (2016), Xu et al. (2017, 2021), Liu et al. (2021), Janssens (2022) and Versluis et al. (2024a). Pochet et al. (2016) address the topic of moving-block (CBTC) conflict detection and resolution by applying a model predictive control approach on a suburban railway network. Without notion of speed, few practical scenarios of disturbed operations are optimised in terms of punctuality. The approach is incorporated in a microscopic simulation tool of the French train operator SNCF. The works of Xu et al. (2017) and Liu et al. (2021) are in the context of the Chinese high-speed railways with homogeneous traffic under fixed-block distance-to-go signalling (CTCS-3). Both propose disjunctive MILP formulations, with Xu et al. (2017)'s model being based on the alternative graph model underlying ROMA (D'Ariano, 2008). Xu et al. (2017) considers speed-dependent train

separation, with a discrete set of speed levels included in an extension (Xu et al., 2021), similar to the modelling of speed by Liu et al. (2021). Janssens (2022) also takes the ROMA model formulation as starting point, extending the alternate graph model to describe moving-block operations. Actually, an approximation of moving block by considering fixed blocks of train length is proposed — without a notion of speed or rerouting options. That leaves our previously mentioned work leading to a fixed-block distance-to-go rescheduling model (Versluis et al., 2024a). More specifically, a conflict detection and resolution model for ETCS Level 2 with TTD obtained from the original RECIFE-MILP model for conventional fixed-block signalling. The presented MILP model considers speed-dependent train separation, given two speed profile options related to maximum or scheduled speed. The combination of a disjunctive MILP model with commercial solver makes it hard to prove optimality of solutions. However, the real-time performance is shown to be acceptable.

For more information, we refer to the review papers of Cacchiani et al. (2014) and Versluis et al. (2024b). In the latter, research gaps an challenges related to the modelling of conflict detection and resolution under moving-block signalling are identified, and research steps to address those are proposed. These include the investigation of the approximation of moving-block operations by fixed-block distance-to-go with a fine discretisation of the track.

2.2. Track discretisation in railway signalling

Track discretisation has been previously studied in the literature, primarily focusing on capacity improvement. Recently, ETCS HTD has renewed research interest in this area. The virtual subsection lengths typically considered for ETCS HTD are 25 to 500 m (Knutsen et al., 2024). The minimum length of 25 m is put forward in the ETCS HTD specification document as the length that should provide a capacity similar to a moving-block system (EEIG ERTMS Users Group, 2024). This is somewhat in contrast to the assertion by Furness et al. (2017), who state that with virtual block or subsection lengths of 200 m, moving-block performance can be achieved, assuming speeds of circa 160 km/h on the open track.

The impact of the section length on the railway (signalling) system is typically considered in terms of (static) capacity. While Knutsen et al. (2024) consider several performance indicators to measure capacity effects, capacity consumption/occupation rate is typically considered as key performance indicator. That goes, for example, for the impact assessment studies of Jansen (2019) and Vergroesen (2020). In both works, the capacity impact of virtual section lengths on ETCS HTD is assessed using simulation. Jansen (2019) considers virtual subsection lengths of 500 m and 100 m, which lead to a decrease in capacity consumption compared to the legacy (fixed-block) system of 16.2% and 20.1%, respectively. Guided by the requirements of the Dutch infrastructure manager ProRail, it was proposed to have section lengths of 200 m with 100 m only at critical infrastructure. Interestingly, this work also includes a test analysis of some simple delay scenarios, i.e., a single train having a 10- or 30-min departure delay. Serious decreases in secondary delay and also significantly shorter recovery times are reported for ETCS HTD compared to the legacy system. The benefits of the smaller section lengths are much smaller, but still significant with ca. 15% decrease in secondary delay and 2% to 10% decrease in recovery time. We note that only retiming is applied, no reordering or rerouting. Building upon the work of Jansen (2019), Vergroesen (2020) specifically considers the impact on ETCS HTD in combination with automatic train operation (ATO). By subdividing TTD sections into virtual (sub)sections, the occupation rate is reduced by 16 percent point.

Cuppi et al. (2021) and Ranjbar et al. (2022) assess the capacity benefits of ETCS HTD in Italian and Swedish studies, respectively. Cuppi et al. (2021) consider virtually dividing the existing blocks of the Roman railway node into subsections with lengths of 350 to 450 m. From a simulation-based comparison with the current multi-aspect signalling system, capacity increases of 56% minimum are reported for the stations in the area. Ranjbar et al. (2022) compare the capacity consumption of ETCS HTD with ETCS Level 2 with TTD and the Swedish legacy signalling system on a single line with homogeneous traffic. For ETCS HTD with virtual subsection lengths of 100 to 20 m, microscopic simulation showed 9% and 14% capacity gain compared to ETCS Level 2 with TTD and the legacy system, respectively. The authors propose further analysis of the effects of ETCS HTD with heterogeneous traffic considering delays as future work.

We conclude that the effects of track discretisation on capacity under virtual-block signalling are well-established. However, to the best of our knowledge, no more than preliminary work can be reported about the consequent effects of track discretisation on conflict detection and resolution.

3. Methodology

With the aim to obtain a conflict detection and resolution model for next-generation distance-to-go signalling such as ETCS Level 2 with onboard TIM, we build upon the earlier presented conflict detection and resolution model for fixed-block distance-to-go signalling (Versluis et al., 2024a). The further development of the model is captured in three steps. First, we introduce the ETCS Level 2 with onboard TIM signalling parameters and their relation with the minimum train separation in Section 3.1. Second, we address the track discretisation granularity by presenting a ‘rediscretisation procedure’ departing from the existing track description in Section 3.2. Third, in Section 3.3, we propose a reformulation of the blocking time constraints for switch areas to better align with the short train separation under next-generation distance-to-go signalling.

3.1. Train blocking times for ETCS level 2 with onboard TIM

The signalling system in place determines the safe train separation. A well-known concept for the modelling of minimum train separation is blocking time theory (Hansen and Pachl, 2014). The blocking time components are setup, reaction, approach, running, clearing and release time. Fig. 2 illustrates the relation between the blocking time components and the minimum train separation under fixed-block distance-to-go signalling, for a specific section.

The setup time is the time required to set a route, to update the MA and translate it into a dynamic speed profile on the driver machine interface onboard. This time is dependent on the type of section that is requested. Specifically, whether the section contains a switch that possibly needs to be set and locked or not. In either case, there is a value to be derived as minimum setup time. For that value, the following subcomponents of the setup time are considered: the trackside processing time, the trackside-to-train communication time and the onboard computation time. Under ETCS, these subcomponents correspond to the radio block centre (RBC) processing time, the RBC-to-train communication time and the European Vital Computer (EVC) computation time. From PERFORMINGRAIL (2022), we obtain the respective values of 0.5 s, 1.0 s and 1.5 s.

For switch sections, the minimum setup time does not suffice given the additional safety requirements concerning movable track elements. Therefore, we consider the following two additional subcomponents: the switch position evaluation time and the switch turning time. The first component captures the time needed to verify the position in which it is set, which is around 1 s. The position evaluation time is in place in all cases of a train requesting a route over a switch. The second component captures the time needed for a switch to be set in the required position. In practice, different types of switches have a different turning time, ranging from (at least) 3 up to 16 s for high-speed switches. The switch turning time is practically only in place in case a train requests a route over a switch that is set in the wrong position. We derive a switch turning time of 6.0 s as representative value as it corresponds to the most common type of switch.

The reaction time is the time from the moment the updated speed profile appears on the driver machine interface until the train starts to decelerate after the train driver has applied the brakes, if needed. Hence, it includes a subcomponent for driver reaction time as well as an additional brake build-up time. Given this split, we obtain 12.0 s as value for the reaction time. That is, 8.0 s for the driver reaction time (PERFORMINGRAIL, 2022) and 4.0 s for the brake build-up time (European Railway Agency, 2020).

The approach time is the time for the train to run from the braking point to the EoA. More specifically, it is the time to run over the braking distance (plus an additional safety margin), as also visualised in Fig. 2. This distance-to-go approach distance, with its speed- and train-dependency, is formalised in Versluis et al. (2024a).

The running time and the clearing time together represent the physical occupation time of the train on the section. As first occupation time component, the running time captures the time to run from the entry to the exit of the section with the front of the train. Subsequently, the clearing time is the time from the moment the front of the train exits the section until the rear of the train exits as well. The occupation time is not directly affected by the signalling principles. However, the running time is clearly dependent on the speed and the featured length of the sections.

The release time is the time from the moment a section is physically cleared by a train until it can be set for another train. Hence, the release time relates to the detection and the communication of the section clearance. In this component, there is a difference between ETCS Level 2 with TTD and with onboard TIM due to the replacement of track-side train detection with onboard train position and integrity monitoring. In line with Shift2Rail (2023), we assume the implementation of Global Navigation Satellite System (GNSS) as train localisation technology. Based on PERFORMINGRAIL (2022), we obtain 2.0 s as GNSS-based release time. This value is derived from the train positioning report (TPR) update time of 1.0 s and the train-to-trackside, i.e., train-to-RBC,

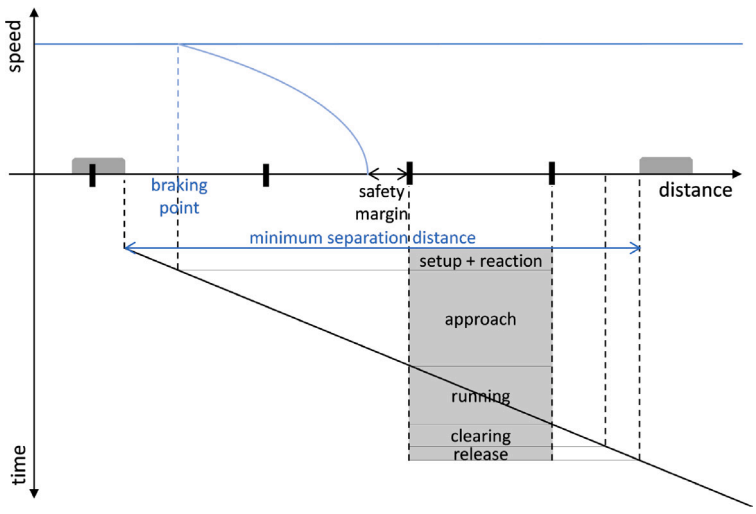

Fig. 2. Blocking time components related to minimum train separation under fixed-block distance-to-go signalling.

Table 1
ETCS Level 2 with onboard TIM parameter values for train blocking times.

Component	Value
Minimum setup time	*3.0* s
Trackside processing time	0.5 s
Trackside-to-train communication time	1.0 s
Onboard computation time	1.5 s
Switch setup time	*1.0* s/*7.0* s
Switch position evaluation time	1.0 s
Switch position turning time	6.0 s
Reaction time	*12.0* s
Driver reaction time	8.0 s
Brake build-up time	4.0 s
Release time	*2.0* s
GNSS-based TPR update period	1.0 s
Train-to-trackside communication time	1.0 s

communication time of 1.0 s. Note that the TPR contains both train position and train integrity information. Table 1 summarises the ETCS Level 2 with onboard TIM parameters and their values relevant for the train blocking times.

3.2. Track discretisation

As introduced in Section 1, the minimum train separation under fixed-block distance-to-go signalling depends on the track discretisation. Given that we build upon a model describing ETCS Level 2 with TTD, we consider the existing track discretised into TTD sections, which we simply refer to as *sections*. In practice, these sections have varying lengths, for example ranging from 35 to 2424 m and from 100 to 2217 m within the control areas presented in Section 4.1. However, for next-generation distance-to-go signalling systems such as ETCS HTD, virtual section lengths in the range of 25 to 500 m are commonly considered (Section 2.2).

We propose a procedure to virtually discretise the existing track into shorter sections based on the sections in place (see Algorithm 1). Sections exceeding a given maximum length are discretised into subsections of equal length. The number of subsections is determined by the ratio of the original section length over the maximum length, rounded up to the nearest integer. This ensures that subsection lengths are between half the maximum length and the maximum length. For *switch sections*, i.e., sections containing a switch, the original sections are kept to ensure compliance with safety regulations. Given the varying section lengths, the resulting discretisation will also be non-uniform. However, we obtain a more uniform discretisation than originally.

Algorithm 1 Track discretisation procedure.

Input: original sections, switch sections, maximum length $l_{\max}$
Output: discretised sections
for all original sections **do**
  if original section is not a switch section and section length $> l_{\max}$ **then**
    $n = \lceil$ section length $/\ l_{\max} \rceil$ {*number of subsections*}
    $l =$ section length $/\ n$ {*subsection length*}
    discretise original section into n subsections of length l
  end if
end for

For illustration of the track discretisation procedure, we consider a fictive double-track line, as shown in Fig. 3. The line connects two switch areas on the left and right, with a side track around a station platform. The bottom track features original sections with lengths of around 600 m, while the top and side track feature original sections of around 360 m. We apply the discretisation procedure given two different maximum lengths: 400 m and 200 m. For the 400-m maximum length, only the original sections on the bottom track between the switch areas are longer and therefore discretised into two subsections of 300 m each (see Fig. 3(a)). For the 200-m maximum length, all non-switch sections are discretised. The sections on the bottom track are divided into three subsections of 200 m each, while the ones on the top and side track are divided into two subsections of 180 m each (see Fig. 3(b)).

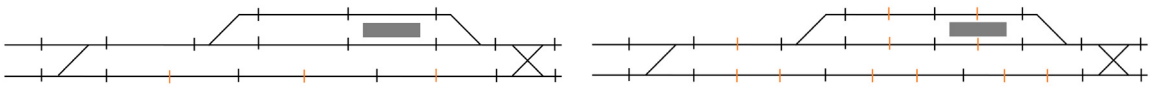

(a) Discretisation for maximum length $l_{\max} = 400$ m. (b) Discretisation for maximum length $l_{\max} = 200$ m.

Fig. 3. Illustration of track discretisation procedure, with original section boundaries in black and additional section boundaries due to discretisation in orange.

3.3. Train separation at switches

In the modelling of train separation, we need to differentiate between sections with and without a switch (Versluis et al., 2024a). Recalling that train separation is modelled in terms of train blocking times, we know from Section 3.1 that a main difference between switch and non-switch sections lies in the switch setup time. For ease of the formulation (see Section 3.3.2), only the minimum setup time is considered in the blocking times. The switch setup time is, instead, included as an additional blocking time component.

In the following, the reformulation of train separation for switches is presented. First, the new and other relevant model components are introduced (Section 3.3.1). Subsequently, the constraints related to the train blocking times are described (Section 3.3.2) Finally, the model objective function is recalled (Section 3.3.3).

The model formulation of the earlier version of the ETCS Level 2 with TTD conflict detection and resolution model as presented in Versluis et al. (2024a) is included in Appendix A. In the model, we consider track locations, i.e., the entry points of track sections, rather than track sections themselves. Here, we provide a brief description of the model's main ideas and concepts. The model considers two speed profile options in line with the scheduled and maximum speed. With a preference for the former through the penalisation in the model objective of the latter, the speed profiles are assigned to trains per stretch of track between switch areas along their route. Hence, trains can only transition between speed profile options after switch areas where speed is limited and assumed to be the same for the two speed options. The speed profile option assigned affects the train running and clearing times on non-switch sections. The running and clearing times together form the (physical) occupation time. The model allows for an extension of the occupation time if it is not possible to exactly adhere to a specific speed profile, including station dwell times. Similar to how the speed profile options are assigned, train orderings are fixed on the level of track stretches, namely per sequence of track sections that are shared by the routes of a pair of trains.

3.3.1. Sets, parameters and variables

To update the MILP model in line with the assumptions, new notation is introduced, see Table 2. For a description of the previously defined sets, parameters and variables, we refer to Versluis et al. (2024a). Here, we describe the new elements, categorised in the three type classes.

First, we introduce two subsets of routes for switch locations, i.e., the entry points of sections containing a switch. R_l^0 contains the routes using the switch in straight position 0, and R_l^1 contains the routes using the switch in diverging position 1.

Second, we introduce two parameters related to the switch setup time. sw^{eval} indicates the time it takes to evaluate the position of a switch, while sw^{turn} represents the time needed to turn a switch from one position to the other. Regarding the switch turning time, we assume the simultaneous turning of switches that are set together under the route-locking interlocking system.

Table 2
Notation for updated blocking time constraints.

Element	Description
T	Ordered set of trains
R	Set of routes
L	Set of locations
$L_t \subset L$	Set of locations which can be used by train $t \in T$
$OL_{t,r,l} \subset L^r$	Set of locations along route $r \in R_t$ such that if train $t \in T$ starts occupying it, the train has not yet cleared location $l \in L^r$, $l \notin OL_{t,r,l}$
$\hat{L}_{t,t',l} \subset L$	Set of locations $l' \in L_t \cap L_{t'}$ which may be used by both trains $t, t' \in T$ such that if t precedes t' on l, then t precedes t' also on l'
$\sigma_{r,l} \in L^r$	Succeeding location of location $l \in L^r$ along route $r \in R$
$\rho_{r,l} \in \mathrm{P}^r$	Speed assignment location associated with location $l \in L^r$ along route $r \in R$
$s_l \in \{0,1\}$	$= 1$ if location $l \in L$ lies in a switch area
$for_{r,l} \in \mathbb{R}_+$	Formation time, i.e., setup and reaction time, of location $l \in L^r$ along route $r \in R$
$rel_{r,l} \in \mathbb{R}_+$	Release time of location $l \in L^r$ along route $r \in R$
$\Delta ct_{t,r,l} \in \mathbb{R}_+$	Additional clearing time for train $t \in T$ of location $l \in L_t$ along route $r \in R_t$ in case of scheduled speed profile
$ref^{\mathrm{s}}_{t,r,l} \in L^r$	Reference brake location for location $l \in L^r$ along route $r \in R_t$ for train $t \in T$ approaching according to scheduled speed profile
$ref^{\mathrm{m}}_{t,r,l} \in L^r$	Reference brake location for location $l \in L^r$ along route $r \in R_t$ for train $t \in T$ approaching according to maximum speed profile
$lag^{\mathrm{s}}_{t,r,l} \in \mathbb{R}_+$	Time by which blocking of location $l \in L^r$ by train $t \in T$ running according to scheduled speed profile along route $r \in R_t$ can be postponed after passing $ref^{s}_{t,r,l}$
$lag^{\mathrm{m}}_{t,r,l} \in \mathbb{R}_+$	Time by which blocking of location $l \in L^r$ by train $t \in T$ running according to maximum speed profile along route $r \in R_t$ can be postponed after passing $ref^{m}_{t,r,l}$
$M \in \mathbb{R}_+$	A large constant
$y_{t,t',l} \in \{0,1\}$	$= 1$ if train $t \in T$ blocks location $l \in L_t \cap L_{t'}$ before train $t' \in T$
$x_{t,r} \in \{0,1\}$	$= 1$ if train $t \in T$ uses route $r \in R_t$
$v^{\mathrm{s}}_{t,r,l} \in \{0,1\}$	$= 1$ if train $t \in T$ passes speed assignment location $l \in \mathrm{P}^r$ along route $r \in R_t$ according to scheduled speed profile
$o_{t,r,l} \in \mathbb{R}_+$	Occupation starting time of train $t \in T$ on location $l \in L^r$ along route $r \in R_t$
$o^+_{t,r,l} \in \mathbb{R}_+$	Extended occupation time of train $t \in T$ between locations $l \in L^r$ and $\sigma_{r,l} \in L^r$ along route $r \in R_t$
$b^{\mathrm{s}}_{t,l}, b^{\mathrm{e}}_{t,l} \in \mathbb{R}_+$	Time at which train $t \in T$ starts/ends blocking location $l \in L_t$
New notation	
$R^i_l \in R$	Set of routes over switch location $l \in L$ requiring position $i \in \{0,1\}$
$sw^{eval} \in \mathbb{R}_+$	Switch position evaluation time
$sw^{turn} \in \mathbb{R}_+$	Switch position turning, i.e., setting and locking time
$I_{t,t',l} \in \{0,1\}$	$= 1$ if trains $t, t' \in T$ are assigned routes that use common switch $l \in L_t \cap L_{t'}$ in opposite position

Third, we introduce binary variables related to required switch positions. $I_{t,t',l}$ indicates whether trains $t, t' \in T$ are assigned routes that use common switch l in opposite position. Note that these 'indicator' variables are auxiliary variables as their values directly follow from the values of the route assignment variables.

3.3.2. Constraints

Constraints (1) to (9) are the model constraints related to the train blocking times. They can be classified into four categories as follows. Constraints (1) to (3) are the start and end blocking constraints. Constraints (4) and (5) are the original disjunctive constraints, now only for non-switch locations. Constraints (6) and (7) are the disjunctive constraints for switches. Constraints (8) and (9) are the 'indicator' constraints.

$$b^{\mathrm{s}}_{t,l} \leq \sum_{\substack{r \in R_t: \\ l \in L^r}} \left(o_{t,r,ref^{\mathrm{s}}_{t,r,l}} + \left(lag^{\mathrm{s}}_{t,r,l} - for_{r,l} \right) x_{t,r} \right) \qquad \forall t \in T,\ l \in L_t, \tag{1}$$

$$b^{\mathrm{s}}_{t,l} \leq \sum_{\substack{r \in R_t: \\ l \in L^r}} \left(o_{t,r,ref^{\mathrm{m}}_{t,r,l}} + \left(lag^{\mathrm{m}}_{t,r,l} - for_{r,l} \right) x_{t,r} + M\, v^{\mathrm{s}}_{t,r,\rho_{r,ref^{\mathrm{s}}_{t,r,l}}} \right) \qquad \forall t \in T,\ l \in L_t, \tag{2}$$

$$b^{\mathrm{e}}_{t,l} = \sum_{\substack{r \in R_t: \\ l \in L^r}} \left(o_{t,r,\sigma_{r,l}} + \left(ct_{t,r,\sigma_{r,l}} + rel_{r,\sigma_{r,l}} \right) x_{t,r} + \Delta ct_{t,r,\sigma_{r,l}} v^{\mathrm{s}}_{t,r,\rho_{r,\sigma_{r,l}}} + \sum_{\substack{l' \in L^r: \\ l' \in OL_{t,r,\sigma_{r,l}}}} o^{+}_{t,r,l'} \right) \qquad \forall t \in T,\ l \in L_t, \tag{3}$$

$$b^{\mathrm{e}}_{t,l} - M\,(1 - y_{t,t',\hat{l}}) \leq b^{\mathrm{s}}_{t',l} \qquad \forall t, t' \in T, t \prec t',\ l, \hat{l} \in L_t \cap L_{t'} : l \in \hat{L}_{t,t',\hat{l}} \wedge s_l = 0, \tag{4}$$

$$b^{\mathrm{e}}_{t',l} - M\, y_{t,t',\hat{l}} \leq b^{\mathrm{s}}_{t,l} \qquad \forall t, t' \in T, t \prec t',\ l, \hat{l} \in L_t \cap L_{t'} : l \in \hat{L}_{t,t',\hat{l}} \wedge s_l = 0, \tag{5}$$

$$b^{\mathrm{e}}_{t',l} - M\,(1 - y_{t,t',\hat{l}}) \leq b^{\mathrm{s}}_{t,l} - sw^{eval} \left(\sum_{r \in R^0_l \cap R^1_l} x_{t,r} + \sum_{r' \in R^0_l \cap R^1_l} x_{t',r'} - 1 \right) - sw^{turn}\, I_{t,t',l}$$
$$\forall\, t, t' \in T, t \prec t',\ l, \hat{l} \in L_t \cap L_{t'} : l \in \hat{L}_{t,t',\hat{l}} \wedge s_l = 1, \tag{6}$$

$$b^{\mathrm{e}}_{t',l} - M\, y_{t,t',\hat{l}} \leq b^{\mathrm{s}}_{t,l} - sw^{eval} \left(\sum_{r \in R^0_l \cap R^1_l} x_{t,r} + \sum_{r' \in R^0_l \cap R^1_l} x_{t',r'} - 1 \right) - sw^{turn}\, I_{t,t',l}$$
$$\forall\, t, t' \in T, t \prec t',\ l, \hat{l} \in L_t \cap L_{t'} : l \in \hat{L}_{t,t',\hat{l}} \wedge s_l = 1, \tag{7}$$

$$I_{t,t',l} \geq \sum_{r \in R^0_l} x_{t,r} + \sum_{r' \in R^1_l} x_{t',r'} - 1 \qquad \forall\, t, t' \in T, t \prec t',\ l \in L_t \cap L_{t'} \wedge s_l = 1, \tag{8}$$

$$I_{t,t',l} \geq \sum_{r \in R^1_l} x_{t,r} + \sum_{r' \in R^0_l} x_{t',r'} - 1 \qquad \forall\, t, t' \in T, t \prec t',\ l \in L_t \cap L_{t'} \wedge s_l = 1. \tag{9}$$

Constraints (1) to (3) are the start and end blocking constraints. Constraints (1) and (2) describe the speed-dependent blocking starting times of track locations per train. Note that the track locations refer to the entry points of sections, as introduced in Versluis et al. (2024a). Constraints (1) ensure that, when a train is approaching a location according to a scheduled speed profile, the location is blocked for that train at the latest the setup and reaction (together 'formation') time before the train passes the 'scheduled-speed' braking distance plus a safety margin. This is captured by the start occupation time of the route-dependent 'scheduled-speed' brake reference location $ref^{\mathrm{s}}_{t,r,l}$ and the corresponding reservation lag time $lag^{\mathrm{s}}_{t,r,l}$. Similarly, Constraints (2) ensure the timely blocking in case of a maximum speed profile. With the 'maximum-speed' braking point lying before the 'scheduled-speed' braking point, a big-M term is added to relax the constraint in case of a scheduled speed profile. We set the same start blocking constraints for all locations, independently of the presence of switches. We note that this is different from Versluis et al. (2024a), where the start of blocking of 'succeeding switch locations' is set together with the preceding switch location's blocking starting time. Constraints (3) set the blocking ending times. The blocking of a location lasts until the train has fully passed the succeeding location along its route, plus the release time. In line with that, the speed-dependent clearing time is included in the blocking time. Additionally, if the train is long enough to keep occupying a location when the front is at the end of the following ones (included in set $OL_{t,r,l}$), also the extended occupation times of the train for these locations has to be accounted for.

Constrains (4) and (5) are the disjunctive ordering constraints for non-switch locations. With these disjunctive constraints, it is decided which of a pair of trains is passing first. They are the disjunctive constraints as they were set for all locations in the original RECIFE-MILP model for fixed-block as well as in the enhanced ETCS Level 2 with TTD version. With these constraints, it is ensured that the blocking times of a location by any pair of trains do not overlap.

Constraints (6) and (7) are the disjunctive ordering constraints for switch locations. The original disjunctive constraints are updated to capture the earlier introduced switch blocking time variants. Beforehand, we note that the constraints are only more restrictive than the original constraints for the combination of a train pair and a switch location if both trains are assigned routes that use the switch. This follows from the values of the 'switch parameter factors', i.e., the 'switch turning' indicator $I_{t,t',l}$ and the 'switch evaluation' expression $\sum_{r \in R^1_l \cap R^2_l} x_{t,r} + \sum_{r' \in R^1_l \cap R^2_l} x_{t',r'} - 1$. If it is not the case that both trains use the location, the indicator takes value 0 and, hence, the switch setting and locking time is dismissed. Similarly, then the expression will be at most 0, with which the switch position evaluation time is effectively cancelled out. In case both trains use the switch, then the switch evaluation time is added as separation of the train blocking times. The 'switch evaluation' expression will equal 1 as both trains then have

a route assigned that uses the switch in either position 0 or 1. In case both trains use the switch in different positions, then also the switch turning time is added because if so, the switch turning indicator takes value 1. If the trains use the switch in the same position, the additional switch separation times is solely the position evaluation time as the indicator's value is 0.

Constraints (8) and (9) ensure that the 'switch turning indicator' takes the right value. Constraints (8) sets the indicator value to 1 if trains t and t' are assigned routes that use switch l in positions 0 and 1, respectively, and Constraints (9) if vice versa.

3.3.3. Objective function

The main objective of the conflict detection and resolution model is to minimise the total delay. Additionally, we want to enforce the assignment of scheduled speed profiles where possible. In the formulation of the objective function, we make use of the following notation. The sets T, S_t, R_t and P^r contain respectively the trains, the stations where train $t \in T$ has a scheduled stop, the routes which can be used by train $t \in T$, and the speed assignment locations along route $r \in R$. The auxiliary variables $z_t \in \mathbb{R}_+$ and $z_{t,s} \in \mathbb{R}_+$ capture the final delay and the delays at scheduled stop $s \in S_t$ of train $t \in T$, while decision variable $v^{\mathrm{m}}_{t,r,l} \in \{0,1\}$ indicates whether or not train $t \in T$ runs according to the maximum speed profile over speed assignment location $l \in P^r$ along route $r \in R_t$. With this notation, the objective function is formulated as follows:

$$\text{minimise} \quad \sum_{t \in T} \Big((z_t + \sum_{s \in S_t} z_{t,s}) + \sum_{\substack{r \in R_t : \\ l \in P^r}} v^{\mathrm{m}}_{t,r,l} \Big).$$

4. Computational experiments

Computational experiments are carried out with the aim to assess the impact of the track discretisation granularity on the conflict detection and resolution model for ETCS Level 2 with onboard TIM. The assessment is focused on the impact in terms of rescheduling decisions, specifically reordering and rerouting, but also covers computational complexity aspects. For this assessment, six different discretisation granularities are considered. From the original partitioning of the track into TTD sections, alternative descriptions of the infrastructure in terms of shorter sections are obtained by applying the track discretisation procedure presented in Section 3.2. The considered maximum section lengths are 800, 400, 200, 100 and 50 m. These maximum lengths are in line with the commonly considered virtual section lengths in ETCS HTD and ETCS Level 2 VB of 25 to 500 m (Knutsen et al., 2024). 25 m is mentioned as minimum length that provides a capacity comparable to moving block (Knutsen et al., 2024; EEIG ERTMS Users Group, 2024), however, already from 200 m down the performance of ETCS Level 2 VB and MB are expected to be similar due to the communication delays in ETCS (Furness et al., 2017; Knutsen et al., 2024).

The experimental setup and results are presented in the following sections. The two case studies are described in Section 4.1. In Section 4.2, insights into model complexity are obtained by looking into the effects of the number of sections on the model dimensions. Section 4.3 presents the results of the computational experiments for the two case studies. Concludingly, Section 4.4 discusses the rescheduling decisions across the discretisations.

4.1. Case study description

The computational experiments are performed in two case studies representing traffic control areas in France: the Gonesse junction and the Rosny-StEtienne corridor. The Gonesse area is a 17-km-long complex junction north of Paris with dense mixed traffic. Fig. 4(a) provides a schematic representation of the Gonesse junction. The junction area includes 89 TTD sections, 38 of which contain a switch, with lengths ranging from 35 to 2424 m, with a mean of 560 m. The TTD sections are grouped into 79 blocks and 37 routes. The area has no station platforms. The timetable of a weekday includes 336 trains, of which 116 high-speed, 129 conventional, and 91 freight trains, with 5 to 13 route alternatives per train.

The Rosny-StEtienne area is a 68-km-long portion of the Paris-Le Havre line with mixed traffic. Fig. 4(b) provides a schematic representation of the Rosny-StEtienne corridor. The corridor includes 239 TTD sections, 44 of which contain a switch, with lengths ranging from 100 to 2217 m, with a mean of 740 m. The TTD sections are divided over 152 blocks and 169 routes. The area has 10 stations with a total of 39 platforms. The daily timetable features 215 trains, of which 2 high-speed, 122 conventional, 56 freight and 35 empty (including work and test) trains, with 1 to 24 route alternatives each. We note that the Rosny-StEtienne corridor is not a high-speed line, so high-speed trains use the maximum speed of conventional trains.

For both traffic control areas, 25 delay scenarios are obtained from a one-day timetable, where an entry delay between 5 and 15 min is imposed on 20% of the trains. The affected trains and the delays are randomly selected following uniform probability distributions to ensure a variety of delay scenarios following the approaches of Lusby et al. (2013) and Pellegrini et al. (2014). These delay scenarios are considered in a one-hour period, i.e., the peak hour from 18:00 to 19:00. Details of the timetable and delays for the one-hour scenarios in both case studies are given in Table 3. We note that these timetables are actual timetables and hence not designed for ETCS Level 2 with onboard TIM.

In the junction area, 28 trains are scheduled to either enter or start their service between 18:00 and 19:00. Of the 28 trains, there are 12 high-speed, 10 conventional and 6 freight trains. The scheduled paths of these trains are shown in Fig. 5(a). The scheduled headway is generally three minutes, with two-minute headways occurring occasionally. As indicators of the timetable's sensitivity to delays, we report the buffer time, i.e., the minimum time between train blocking times along their shared path, and travel time supplement, i.e., the difference in travel time through the area between running at maximum speed and at scheduled speed. Buffer times of 105 and 40 s are included in the three-minute and two-minute headways, respectively, when evaluated under ETCS Level

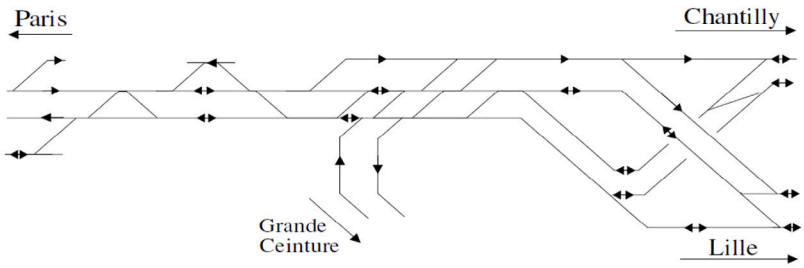

(a) Gonesse junction.

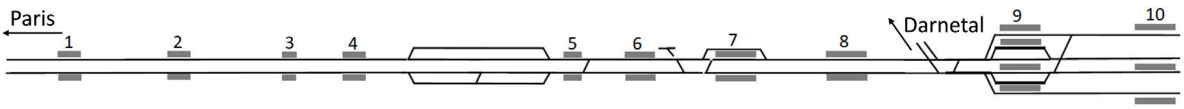

(b) Rosny-StEtienne corridor.

Fig. 4. Schematic track layouts of the considered control areas.

Table 3
Details of the case study scenarios in terms of timetable and delays.

	Junction	**Corridor**
Timetable		
# trains	28	19
- # high-speed trains	12	0
- # conventional trains	10	12
- # freight trains	6	3
- # empty trains	–	4
Scheduled headway	180/120 s	210/270 s
Buffer time	105/40 s	21/73 s
Dwell time supplement	–	10 – 30 s
Travel time supplement	60 s	90 – 150 s
Delays		
# delayed trains - median	6	4
# delayed trains - range	3 – 9	1 – 7
Total delay - range	1244 – 5510 s	693 – 4863 s
Mean train delay - range	415 – 663 s	464 – 817 s

2 with onboard TIM with the original discretisation into TTD sections. The travel time supplement is approximately one minute for all trains.

In the corridor area, 19 trains are scheduled to either enter or start between 18:00 and 19:00. Of the 19 trains, there are 12 conventional, 3 freight and 4 empty trains. The scheduled paths of these trains are shown in Fig. 5(b). The scheduled headway varies significantly, although 3.5 and 4.5 min occur regularly. As for the 'timetable sensitivity indicators' of buffer and supplement times, we report the following. The 3.5-min and 4.5-min headways respectively include 21 and 73 s of buffer time. The dwell time supplements are 10 to 30 s per stop. For the travel time supplement, there is a potential difference in exit time of 1.5 to 2.5 min.

The input delays for the considered hour are directly taken from the delay scenarios defined for the daily timetable. As a result, the number of delayed trains show some variation around the imposed 20%. In the junction case study, the number of delayed trains ranges from 3 to 9, with a median of 6. The total train delay ranges from 1244 to 5510 s, while the mean train delay varies between 415 and 663 s. In the corridor case study, the number of delayed trains ranges from 1 to 7, with a median of 4. The total train delay ranges from 693 to 4863 s, while the mean train delay varies between 464 and 817 s.

4.2. Impact of methodological changes on model size

Before diving into the experimental results, we consider the effects of the methodological changes presented in Section 3 on the model size. As a first step, we consider the number of sections in the six considered track discretisations corresponding to different granularities, as a result from the track discretisation procedure of Section 3.2. Table 4 presents the various number of sections for the two case studies, with the original number of sections (89 and 239, respectively) in the first column. Additionally, Table 4 includes the growth rates. A growth rate indicates the increase in number of sections relative to the number of sections in the one step coarser discretisation. With the maximum section length being halved over the discretisations (from 800 to 50 m), the growth

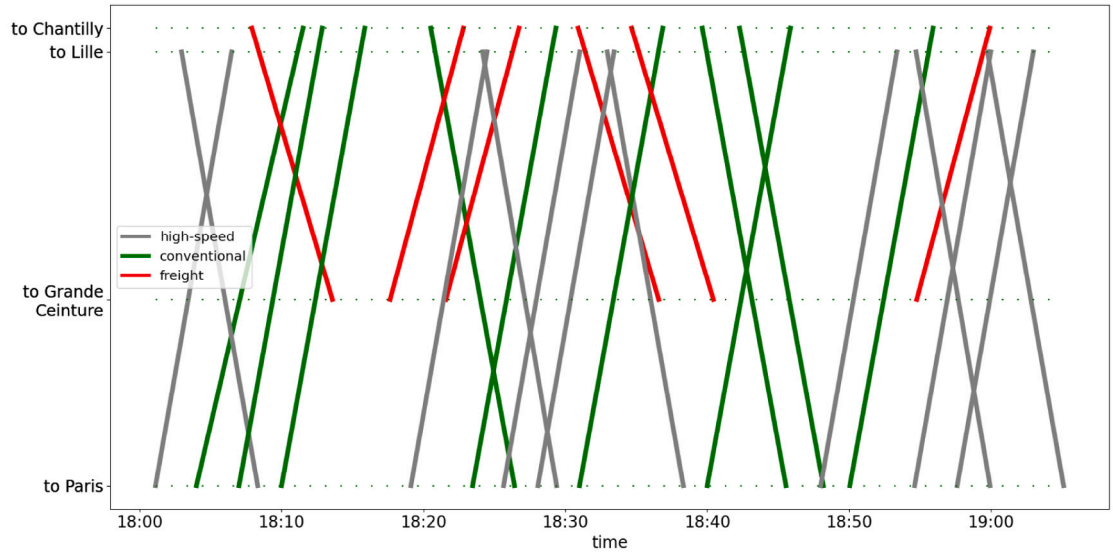

(a) Train path diagram of timetable considered for Gonesse junction.

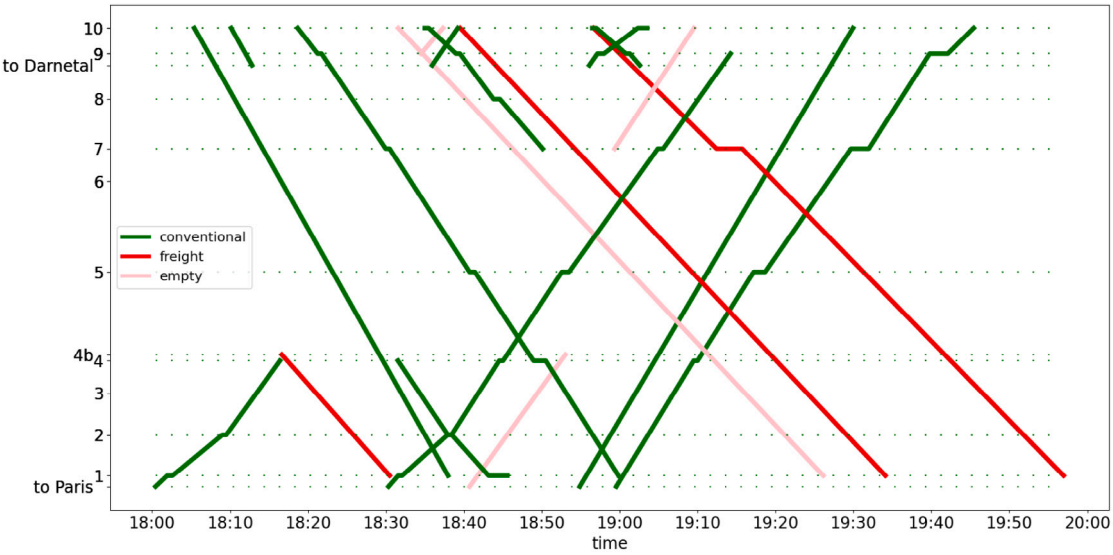

(b) Train path diagram of timetable considered for Rosny-StEtienne corridor.

Fig. 5. Train path diagrams of case study timetables.

Table 4
Number (#) of sections per case study for the different discretisations, represented by their maximum section lengths. In brackets, the growth rate with respect to one step coarser discretisation.

# sections	**Original**	**800 m**	**400 m**	**200 m**	**100 m**	**50 m**
Junction	89	101 (1.13)	135 (1.34)	203 (1.50)	345 (1.70)	630 (1.83)
Corridor	239	340 (1.42)	530 (1.56)	912 (1.72)	1692 (1.86)	3252 (1.92)

rate is maximum two. A rate of two will, however, not be reached given that both case studies contain switches whose sections are never split.

The finer the discretisation, the closer the growth factor gets to two as more sections need to be split that have not yet been split due to their original length being shorter than the previously considered maximum length. So, it shows the presence of a significant amount of original sections with a length even shorter than 50 m. Also, we see a remarkable difference between the two case studies. Not only the original number of sections is much higher in the corridor than in the junction area, but also the growth rate. The

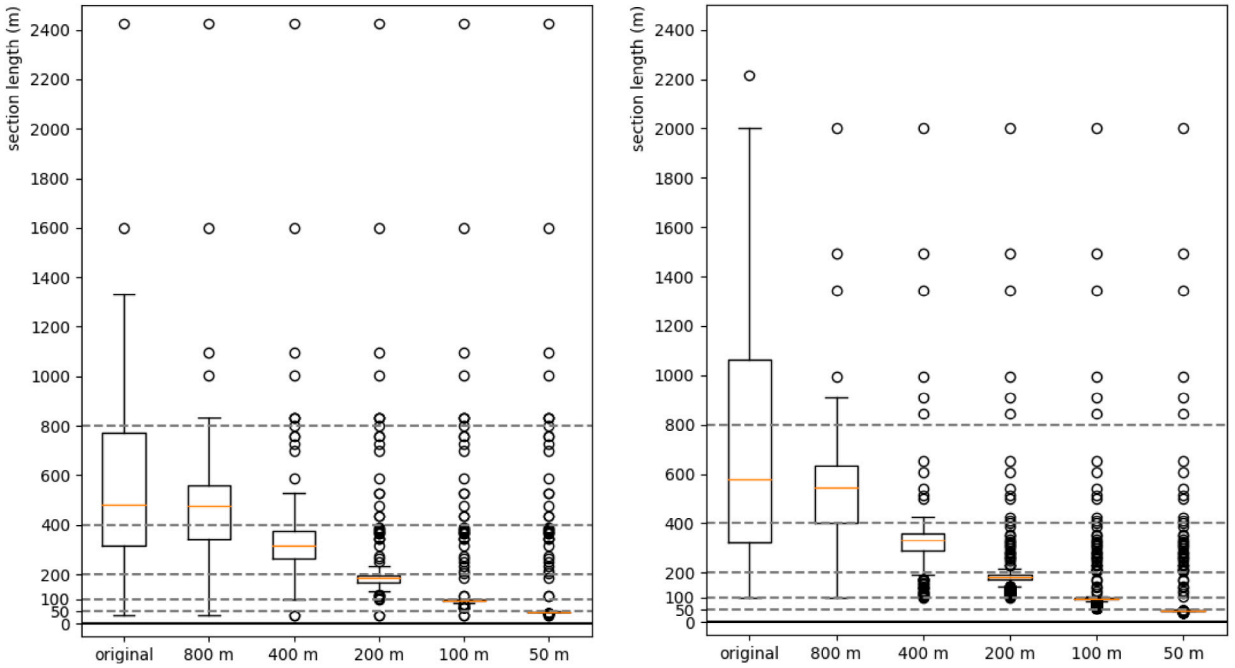

(a) Junction. (b) Corridor.

Fig. 6. Distributions of section lengths for the different discretisations in the case studies.

difference in growth rate from, for example, the original length to 800 m shows the relatively high number of sections longer than 800 m in the corridor. This is not surprising given the characteristics of the other area as junction. That is, the junction area has relatively more switch sections and generally shorter sections compared to the corridor area.

The difference in section lengths between the two case studies is illustrated in Fig. 6. The distribution of the section lengths is given for the original track discretisation in terms of TTD sections as well as for the rediscretisations. Figs. 6(a) and 6(b) clearly demonstrate the wide range of section lengths in the original representation of the junction (35 to 2424 m) and corridor case study (100 to 2217 m), respectively. Due the original section lengths averaging between 500 and 600 m, the median section lengths are practically the same in the 800-m discretisation. In the finer discretisations, this median value decreases significantly. The median value stays below the maximum discretisation length, despite not splitting (long) switch sections, which is clearly visible by the spread in the section length beyond the maximum discretisation length. That is due to the limited amount of switch sections, originally short sections, and the fact that by the discretisation procedure, the sections are split into subsections with lengths between half the maximum and the maximum length.

Related to the section lengths, we include notes on the section length variability and the switch sections. Overall, the variation in section lengths within the discretisations make it less straight forward in terms of drawing conclusions. An alternative approach would be to consider uniform section lengths, though in its turn that would not capture the practicality of having shorter sections close to stations and switches, i.e., (capacity) bottlenecks. Moreover, dividing TTD sections into virtual subsections is in line with the ETCS HTD concept. Regarding switch sections, we initially assumed they would be relatively short and therefore did not partition them further. However, we observed some longer switch sections due to extended TTD sections, in which a switch was included without additional boundary partitioning. Since these sections did not emerge as critical in our results, we opted to retain them as they were in our models. Alternatively, these sections could be partitioned into a pure switch section and adjacent TTD sections, where the latter could be partitioned into parts of maximum lengths like the other TTD sections.

With the increase in the number of sections over the discretisations, the dimensions of the mathematical model are negatively affected. This is clearly visible in Table 5, which reports the number of binary variables, continuous variables and constraints of the MILP for the two case studies. While the overall model size increases for finer discretisations, the number of binary variables is stable. The independence of the number of binary variables on the discretisation is explained by the binary model variables being the switch turning indicator variables as addition to the ‘original’ ordering, routing and speed variables, which are (in terms of sections) defined for either a switch or an ‘open line stretch’, see also Versluis et al. (2024a). The increases in numbers of continuous variables and constraints across the discretisations are close to the growth rate of the number of sections as reported in Table 4.

In addition to showing the trends in model dimensions across discretisations, Table 5 highlights the impact of the reformulation of the switch blocking time constraints on the model size. This impact is assessed by comparing the model dimensions using the old and new formulation for the same discretisation. Specifically, we compare the model dimensions from Versluis et al. (2024a) with

Table 5
Number (#) of binary and continuous variables, and constraints of model initialised without delays for the different discretisations.

	Versluis et al. (2024a)	**This work**					
		original	800 m	400 m	200 m	100 m	50 m
Junction							
# binary variables	6 186	12 857	12 857	12 857	12 857	12 857	12 857
# continuous variables	28 844	28 844	32 544	42 202	62 030	102 346	184 221
# constraints	81 407	94 749	105 567	132 452	189 982	304 094	547 369
Corridor							
# binary variables	4 649	5 275	5 275	5 275	5 275	5 275	5 275
# continuous variables	68 902	68 902	97 228	151 210	258 569	480 938	923 402
# constraints	113 214	114 466	159 643	246 042	420 732	782 561	1 502 517

those in this work considering the original section lengths. This comparison tells us that the reformulation leads to a significant increase in the number of binary variables and constraints, while the number of continuous variables are not affected. This is in line with the addition of the switch turning indicator variables and their 'value setting constraints'. Remarkable is the growth rate of the number of binary variables in the junction case study. Indeed, the number of switches is proportional significantly larger (38 out of 89 TTD sections versus 44 out of 239 TTD sections), but the increase in number of constraints is comparable for the two case studies. We do note that in the presolve phase, the model dimensions are already significantly cut down by CPLEX.

4.3. Analysis of conflict detection and resolution model for ETCS level 2 with onboard TIM

The experiments are performed on the two case studies described in Section 4.1 considering two aspects. In Section 4.3.1, the effects of the model adjustments to the earlier presented conflict detection and resolution model are analysed. We compare the (rescheduling) results obtained by, on the one hand, the model for ETCS Level 2 with onboard TIM as presented in Section 3 with, on the other hand, the model describing ETCS Level 2 with TTD, as presented in Versluis et al. (2024a). For this comparison, we fix the track discretisation to correspond to the TTD sections in place.

Subsequently, we assess the impact of the track discretisation on the enhanced conflict detection and resolution model for ETCS Level 2 with onboard TIM. For the junction and the corridor case study, the sensitivity analysis is carried out in two steps, which is addressed in Sections 4.3.2 and 4.3.3, respectively. First, the model is run to find optimised (rescheduling) solutions for the 25 delay scenarios in each of the six discretisations. The solutions are evaluated (and compared) in terms of objective value, computation time, optimality gap and rescheduling decisions. Second, the optimised solutions are cross-evaluated. That is, the solution obtained with a certain discretisation is evaluated given a different discretisation.

The experiments are run on an Intel(R) Xeon(R) CPU Gold 6226R CPU @ 2.90 GHz, 16 cores, 256 GB RAM. The implementation uses IBM ILOG CPLEX Concert Technology for C++, version 20.1. For the optimisation, the computation time limit is set to 3600 s. With this, the time limit does not correspond to a real-time application, but it allows for a thorough evaluation of the model. For an idea on the real-time applicability, we refer to Versluis et al. (2024a). For the earlier model version for ETCS Level 2 with TTD, Versluis et al. (2024a) conclude that despite the difficulties in obtaining optimally proved solutions, the real-time performance is acceptable. Given that the latter is due to the short computation time needed to find high-quality solutions, also for the larger model presented in this paper, reasonable real-time performance can be expected. However, in general, more efficient solution algorithms and/or decomposition need to be considered.

4.3.1. Effects of modelling adjustments on optimisation solutions

In this paper, the fixed-block distance-to-go conflict detection and resolution model of Versluis et al. (2024a) is adjusted to describe ETCS Level 2 with onboard TIM. The two adjustments introduced in Sections 3.2 and 3.3 are directly related to the minimum train separation, being the incorporation of onboard TIM parameter values (such as the GNSS-based train position report update period) and the reformulation of the switch blocking time constraints. With these adjustments, the minimum train separation is modelled differently. On the open line, the train blocking times are shorter. At the switches, however, the train blocking times have increased due to the explicit consideration of the switch setup time. This was needed to differentiate between the route relations to account for general interlocking rules.

In Table 5, we have seen that the new constraints lead to serious increases in the model dimensions, specifically for the junction case study. From the overview of the (mean) results of the models with and without the model adjustments in Table 6, it is clear that the larger model size is directly reflected in the optimisation process. The computation time used on average increases from 782 to 3468 s for the junction and from 377 to 1136 s for the corridor. The increase is significantly larger for the junction, for which also the model size increase was a lot larger. Without the adjustment, the model was able to solve all but two scenarios to optimality within the computation time limit. With the adjustments, only two were solved to optimality. Despite the poor performance in terms of 'optimality convergence', the obtained solutions are of (relatively) good quality — with a maximum optimality gap of 1.01% and a mean gap of 0.22%. We end up with a minimal drop in mean objective value, from 6866 to 6861 s, for the junction area. Underlying, we have that in about 50% of the cases, the ETCS Level 2 with TTD model gives the best objective value and in the other half of the cases the ETCS Level 2 with onboard TIM model does so. The fact that without the model adjustments a better

Table 6
Mean results of model optimisation with (w/) and without (w/o) model adjustments.

	Junction		Corridor	
	w/	w/o	w/	w/o
Objective value	6861	6866	4764	4753
Speed penalty	62	46	16	9
Computation time (s)	3468	782	1136	377
Optimality gap (%)	0.22	0.01	0.01	0.02
# optimal solutions	2	23	19	19

solution can be obtained is due to the addition of the switch setup time. We do remark that the speed component of the objective value, counting the number of times a maximum speed profile is assigned to a train between switches/on an open line track, is larger in the adjusted model. This means that in the total delay of the two solutions, there is some more difference, in favour of the enhanced model.

The corridor case study has similar results, but there are also differences. As a result of the less increased model dimensions, the corridor case study is solved to optimality for the same number of scenarios in the two model versions (19/25). Despite the longer mean computation time, the mean optimality gap is lower (0.01% versus 0.02%). This does not help, as we end up with a mean objective value that is higher for the enhanced model. Here too, there is a higher speed penalty, but also the total delay alone is higher, though minimally. Apparently, the effects of the additional switch setup time is larger here than in the junction. There are more switches, though less relative to the number of sections in the case study.

More relevant is the impact to the modelling of the conflict detection and resolution. We have seen that we get different results for the model versions with and without the adjustments. For conflict detection and resolution, different results would mean different rescheduling decisions. So we also looked into the solutions themselves. For the case study's scenarios, we compared the two solutions in terms of reordering and rerouting decisions.

For the junction scenarios, no solution was the same. At least, one different route was assigned. The number of different routes goes up to 11, while only in one scenario one different order was proposed. Also for the corridor scenarios, only one time one different order was proposed. Differently from the junction, in nine scenarios, the same solution was proposed. In the other cases, one to seven different routes were found.

4.3.2. Impact of track discretisation in the junction case study

In this section, we present and discuss the experimental results for the junction case study. Two key indicators for the optimisation step are the objective value and the optimality gap obtained within the maximum computation time of 3600 s. The trends in objective values and optimality gaps across the solutions obtained with the different discretisations are illustrated in Fig. 7. In Fig. 7(a), the objective values of the 25 scenarios are reported relative to the objective value obtained with the original discretisation, complemented with the median relative objective value. As the model describes a minimisation problem, negative percentages indicate an improvement, while positive percentages indicate worse objective values. On the one hand, Fig. 7(a) tells us that, for the most part, the discretisations of 800, 400, 200 and 100 m lead to an improvement over the original discretisation. On the other hand, the 50-m discretisation often performs worse. Looking at Fig. 7(a), the number of scenarios with a worse performance is already significant for the 100-m discretisation. Given that the shorter the sections the shorter the separation distance, the reason for the worse performance is that the increased model dimensions result in less optimised solutions. As Fig. 7(b) illustrates, the median optimality gaps after the maximum computation time are significant for the two finest discretisations, while the median optimality gaps for the coarser discretisations are relatively close to 0%. However, Fig. 7(b) also shows that the median computation time used is close to the computation time limit from the original discretisation on. Only two scenarios are solved to optimality in the original discretisation. For the 800-, 400-, 200-, 100- and 50-m discretisations, respectively three, one, one, zero and zero obtained solutions are proven to be optimal.

The relatively poor quality of the solutions of the 100- and 50-m discretisation is also clear in Fig. 8, in which the absolute objective values of the cross-evaluation are plotted. That is, the means of the objective values obtained by evaluating a solution optimised for one discretisation in another discretisation. While the lines in the top of the plot correspond to the 100- and 50-m solutions evaluated with the various maximum section lengths, it is the 800-m solution which results in the bottom line. Hence, typically, the 800-m solution is the best throughout the discretisations. Given the small difference in objective value, this is mainly a result from the suboptimality in the case of finer discretisations. Fig. 8 illustrates the trend in objective value across the evaluations of the different solutions in the different discretisations. The overall trend is clear: the finer the discretisation, the lower the objective value of a solution. We note that, for the junction area, the maximum difference in objective values between evaluations of a solution is 21 s, corresponding to a minimal 0.3%. The gain in objective value for a specific solution purely indicates the effect of the shorter train separation due to the shorter sections in a finer discretisation.

At the level of individual scenarios, we do not necessarily see the same trend in objective value of the solution cross-evaluations. Occasionally, a best solution for one discretisation does not yield the minimum objective value observed for another discretisation. In the junction case study, this occurs in seven of the 25 scenarios. Typically in these cases, for the original discretisation a unique best solution is found which performs worse in one or more finer discretisations compared to their optimised solution. We note that this concerns the 800, 400 and 200 m since the 100 and 50 m solution have too large optimality gaps. In turn, the solution

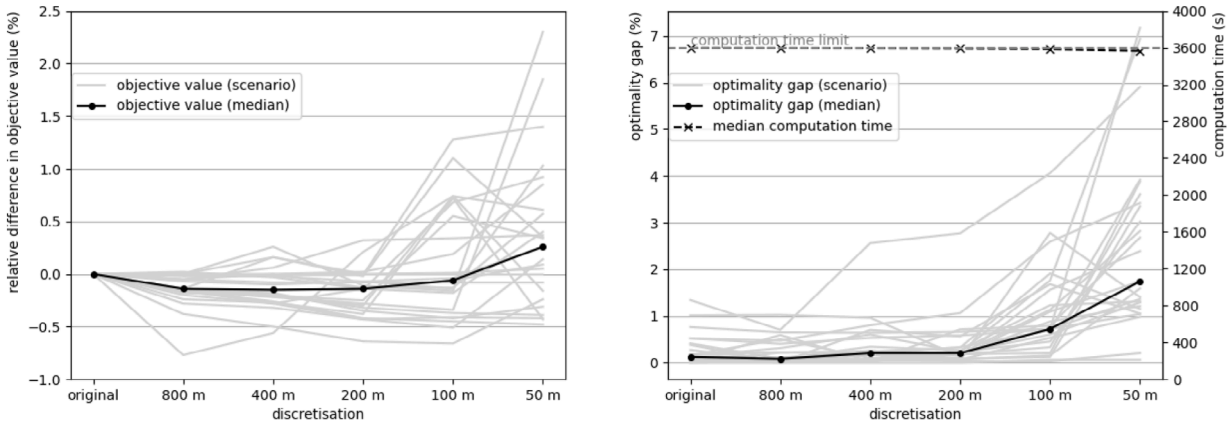

(a) Objective values relative to original ones.

(b) Optimality gaps and computation times.

Fig. 7. Results of the junction case study: trends in objective value and optimality gap across discretisations.

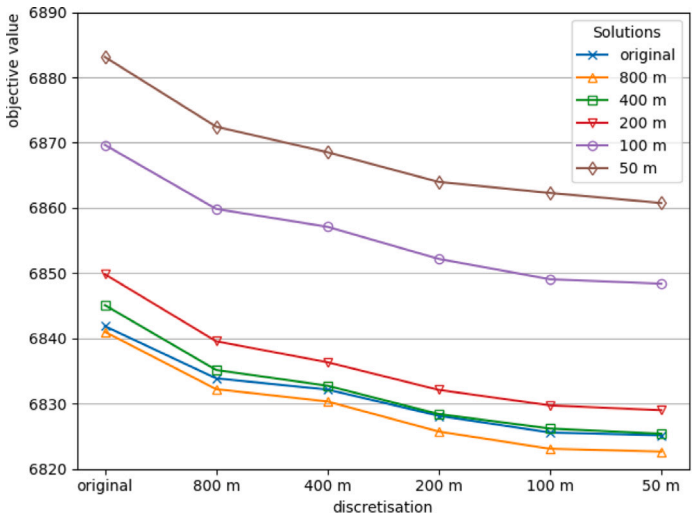

Fig. 8. Mean objective values of optimised solutions evaluated in all discretisations.

optimised for these finer discretisations give a higher objective value than the optimised one in the original discretisation. These differences, both in the original and the finer discretisations, are a matter of a couple of seconds.

Despite these differences being minimal, there is something significant behind it. Underlying these differences are different rescheduling decisions. For the seven scenarios in the junction case study, the differences in decisions are three to nine route assignments. There is an exception, for one scenario there is a different order decided in the exclusively best solutions. That exceptional scenario is also the only one for which the best solution for the original discretisation is not its own solution; the two best solutions are from the 800 and 200 m discretisations. This is possible due to the overall slightly better performance of the 800 m than the original discretisation, which is illustrated by the lowest objective values in the cross-evaluation (Fig. 8) as well as the lower median computation time and optimality gap (Fig. 7(b)).

Concerning the different route assignments, they are sometimes simply the result of a shorter or faster route. In other cases, it is inferred from the interaction between trains. For example, the first train of a conflicting train pair can be detoured in order to allow a free track for the second train. This can go together with a ‘maximum speed assignment’. Typically, the two routing solutions have more effect in the original discretisation than in the finer one. Some of the trains are not affected by the difference in routes in the finer discretisation, while they are in the original discretisation. Note that there is always at least one train for which it does matter in the finer discretisation, otherwise the scenario would not be considered here. The potentials of finer discretisations in terms of conflict detection and resolution are better illustrated by the different train ordering observed. It is an exemplary result of what shorter train separation through shorter sections (in combination with the switch blocking times) can lead to.

Overall, we can conclude that in the considered junction case study, the impact of track discretisation granularity on conflict detection and resolution is limited. This outcome is primarily due to the model's complexity as a result from the model formulation and the traffic density. Additionally, the track layout with relatively many switches reduces the effects. While the overall impact is minimal, there are clear indications of the potential impact of track discretisation granularity on conflict detection and resolution. Notably, the original discretisation into TTD sections does not have the overall best performance in balancing solution quality and computational complexity. Instead, the discretisation with a maximum length of 800 m (and a median length of 500 m) performs better. Looking further, the 200-m discretisation can be a viable option. Due to the high complexity, its performance is unstable, but promising in terms of objective value. With some (more) computational improvement, the 100-m option might also become interesting as there is still some gain to be obtained from 200 to 100 m (see cross-evaluation). For a better assessment, it is essential to reduce the computational complexity of the conflict detection and resolution model.

4.3.3. *Impact of track discretisation in the corridor case study*

For the corridor case study, the trends in objective value and optimality gap across the solutions obtained with the different discretisations are illustrated in Fig. 9, with the objective values relative to the objective value obtained with the original discretisation in Fig. 9(a) and the optimality gaps and used computation times in Fig. 9(b).

Aside from the 50-m discretisation, the median objective values across the discretisations are the same, as a consequence of that being the case for 16 of the 25 scenarios. The higher median objective value for the 50-m discretisation is due to bad performance of one specific scenario with an above-median value in the 50-m discretisation while having below-median values in the other discretisations.

Consequently, the median optimality gap is practically stable at 0% across the discretisations. Only for the 100-m and 50-m discretisations, the median optimality gap increases very slightly. The optimality gap of some individual scenarios starts to increase more significantly from the 400-m discretisation on. This goes hand-in-hand with the rise in the median computation time used, which increases from the 400-m discretisation to become significantly higher for the 200-, 100- and 50-m discretisations.

Fig. 9(a) shows that for all the scenarios that do not have the same objective values across the discretisations, the objective values actually show a decreasing trend except for the 50-m discretisation (up to −4.17%). Hence, for this case study, we see that despite the increasing computational complexity, the results of a discretisation are at least as good as those of the coarser discretisations (with the exception of the 50-m discretisation). Few other exceptions can be found, for example when going from 400 to 200 m. These are the results of suboptimality of the solution obtained for the finer discretisation, as they indeed correspond to the lines in Fig. 9(b) with the increasing optimality gaps.

As Fig. 8 did for the junction case study, Fig. 10 shows the results of the cross-evaluation for the corridor case study. By plotting the mean of the absolute objective values from evaluating the solutions optimised using the different discretisations in the other discretisations, we can (better) assess the 'overall' quality of the obtained solutions. The plot shows three groups of trend lines. The first group consists of the original, the 800- and the 400-m solution, the second one contains the 200- and the 100-m solution, and the third corresponds to the 50-m solution. The three groups describe very similar trends, i.e., the declining decrease in objective value due to shorter train separation when considering finer track discretisations. The difference between them lies in the exact values. The second and third group obtain values slightly (ca. 0.1%) or significantly (ca. 5.5%) higher, respectively, compared to the first group due to the higher suboptimality in the optimisation step for the finer discretisations, visible by both the increased median computation time and the higher number of positive optimality gaps in Fig. 9(b). The limited number of positive optimality gaps for the coarser discretisations results in minimal values in the cross-evaluation. The offset between the groups is the result of

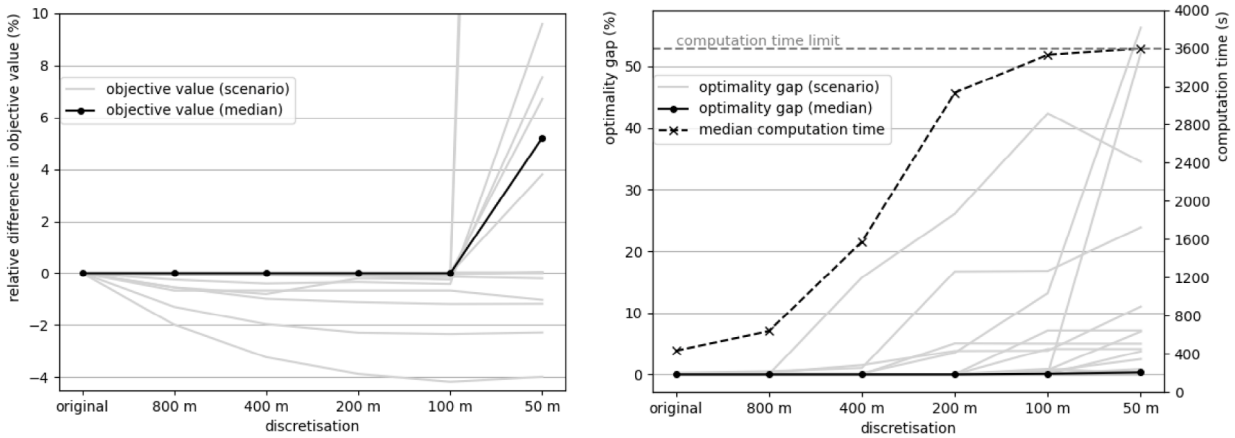

(a) Objective values relative to original ones.

(b) Optimality gaps and computation times.

Fig. 9. Results of the corridor case study: trends in objective value and optimality gap across discretisations.

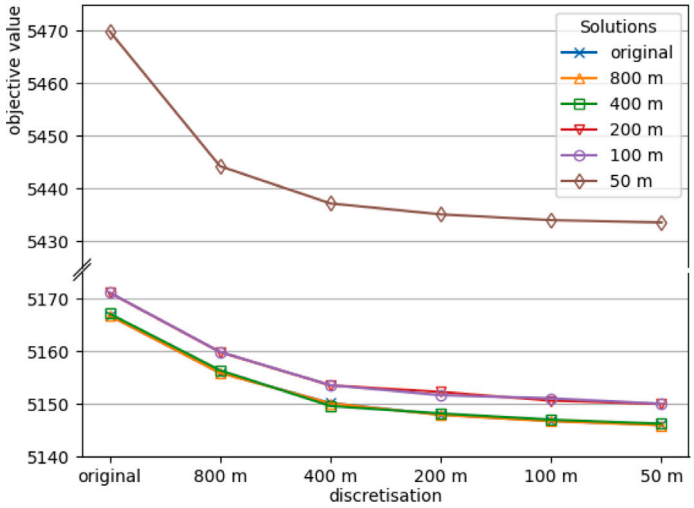

Fig. 10. Mean objective values of optimised solutions evaluated in all discretisations.

a limited number of scenarios for which the final solution for the finer discretisation(s) is worse than the objective value of the evaluation of the other solutions. Within the first group, the 800-m solution is the best by a minimal difference overall. However, for the evaluation in the 400-m discretisation, the 400-m solution proves to be best. Within the second group, it does not hold that the solutions have the lowest objective in their respective discretisation, again due to the couple of scenarios with a worse final objective value. The third group of the 50-m discretisation, does not play a role due to the frequent and significant suboptimality.

For the corridor case study, there is less to say on the level of individual scenarios than in the junction case study. As already said, for 16 of the 25 scenarios, the same objective values are found across the different discretisations. In six of these 16 scenarios, the same rescheduling decisions are proposed, meaning that in the other ten scenarios, alternative solutions of the same quality are found.

There is a second group for which either the same solutions or solutions of the same quality are found. For the six scenarios in this group, the same rescheduling decisions result in different objective values due to the shorter train separation enabled by a finer track discretisation. The gain in objective value reaches up to 4.17%.

This leaves three scenarios to be discussed. For these scenarios, both different objective values and significantly different solutions have been obtained. Unfortunately, in all three cases it holds that the objective value increases for a finer discretisation, meaning that the different solution is a suboptimal solution as a consequence of having a positive final optimality gap.

Given the above classification of the scenarios based on their solutions we have to conclude that for the corridor case study the impact of the track discretisation on conflict detection and resolution is non-apparent in terms of rescheduling decisions. With the mean decrease in objective values over the discretisations being similar to that of the junction case study, we identify track layout and traffic density as indicators for the impact of track discretisation on conflict detection and resolution.

4.4. Discussion of rescheduling decisions for different discretisations

In line with the focus on the effects of track discretisation on rescheduling decisions, we conclude the experimental section with a discussion of how these decisions differ across the considered discretisations for our implementation of ETCS Level 2 with virtual subsections. In Table 7, we provide an overview of the number of proposed reordering and rerouting decisions per discretisation that are different with respect to the decisions proposed for the next coarser one. So, for the 800-m discretisation the comparison is made with the original discretisation, while for the finer discretisations, i.e., 400, 200, 100 and 50 m, it is made with the 800-, 400-, 200- and 100-m discretisation, respectively. Additionally, Table 7 reports the number of scenarios for which the solution was proven optimal, as well as the number of scenarios for which the solution of the considered discretisation was equally good or better in terms of objective value compared to the solution of the next coarser one (when evaluated for the considered discretisation).

A first observation is that the corridor case study appears quite stable with respect to rescheduling decisions. This is evident from having only one scenario for one discretisation with an improved objective value. Furthermore, the number of corridor scenarios with a proven optimal solution is relatively high (up to 19 of 25 compared to up to 3 of 25 for the junction case study), while the number of scenarios with solutions resulting in a worse objective value is relatively low (from 0 to 9 of 25 compared to from 3 to 16 of 25 for the junction case study). In contrast, the junction case study seems more sensitive to discretisation changes. For each discretisation, there are three to seven scenarios for which a better objective value was found due to different decisions compared to the next coarser discretisation.

A second observation is that the number of different routing decisions gives an indication rather than a complete picture of the impact. Not all different route assignments are critical, i.e., contributing to the improvement of the objective value. This is

Table 7
Differences in rescheduling decisions across discretisations in the junction and corridor case study. Indicated are the numbers of differing order and route decisions (# Δ o & r) between subsequent discretisations for scenarios with same or improved objective value.

	# scenarios with proven optimal sol.	**Same objective value**			**Improved objective value**		
		# scenarios	# Δ o & r decisions		# scenarios	# Δ o & r decisions	
			median	mean		median	mean
Junction							
800 (vs orig)	3/25	15/25	0 & 3.5	0 & 3.4	7/25	0 & 7	0 & 6.6
400 (vs 800)	1/25	16/25	0 & 4	0 & 3.6	3/25	0 & 6	0.3 & 6.7
200 (vs 400)	1/25	11/25	0 & 3	0 & 3.4	6/25	0 & 7.5	0 & 7.4
100 (vs 200)	0/25	7/25	0 & 4	0 & 4.8	3/25	0 & 3	0 & 3.7
50 (vs 100)	0/25	3/25	0 & 6	0 & 4.3	6/25	1 & 3.5	0.8 & 4.8
Corridor							
800 (vs orig)	19/25	24/25	0 & 2	0 & 2.5	1/25	1 & 8	1 & 8
400 (vs 800)	15/25	24/25	0 & 4	0 & 3.4	0/25	–	–
200 (vs 400)	14/25	23/25	0 & 3	0 & 2.9	0/25	–	–
100 (vs 200)	6/25	23/25	0 & 3	0 & 2.8	0/25	–	–
50 (vs 100)	0/25	16/25	0 & 0.5	0 & 1.7	0/25	–	–

illustrated by the number of different routes assigned in scenarios with solutions given the same objective value. In the junction and corridor case studies, respectively circa four and three of the route assignments seem to be interchangeable with respect to total train delay. Considering rescheduling practice, in which there is a general reluctance to apply (local) rerouting, introducing a penalty for assigning an alternative route can be included to only allow rerouting if it results in some delay recovery.

Overall, we conclude that for the corridor case study, the 800-m discretisation performs best, as it has a non-negative and even some positive impact on the quality of the solution in terms of rescheduling decisions. While finer discretisations are unlikely to provide further benefits in this context, they also rarely lead to worse outcomes. For the junction case study, the impact of discretisation is less straightforward. Considering both the number of scenarios with an improved objective value and those with a worsened objective value, we conclude that the 800-, 400- or the 200-m discretisations are all valid options.

5. Conclusions

In this paper, we assessed the impact of the track discretisation granularity on conflict detection and resolution for next-generation distance-to-go signalling. The performed assessment considers both the mathematical optimisation model as such and the computational results obtained with it. A particular focus is on the impact on rescheduling decisions included in the model solutions.

The considered conflict detection and resolution model is based on an earlier developed model for fixed-block distance-to-go signalling. The model is updated from European Train Control System (ETCS) Level 2 with trackside train detection (TTD) to ETCS Level 2 with onboard train integrity monitoring (TIM) by considering onboard TIM parameters and introducing a track (re)discretisation procedure. Additionally, as a general update of the model, a reformulation of train separation at switches is considered.

The impact assessment is conducted on two case studies featuring different types of control areas: a heavily trafficked junction and a less densely trafficked corridor. The discretisations considered are derived from the original track partitioning into TTD sections and are characterised by maximum section lengths in the range from 50 to 800 m. These (virtual) section lengths are in line with those commonly considered in research on ETCS Hybrid Train Detection, which currently has the industry's focus.

Over the discretisations, from coarse to fine, the dimensions of the mixed integer linear programming (MILP) model grow linearly with the number of sections. The main increase in model dimensions is, however, due to the reformulation of the train separation constraints at switches. Given the relatively large model dimensions and the exploration phase of the research, a computation time limit of one hour is set. Nevertheless, for the finer discretisations and the junction case study in general, the model is not solved to optimality in most cases.

Regardless of the more frequent suboptimality for the finer discretisations, the corridor case study practically features non-increasing objective values (up to −4.17%). They are, however, solely due to shorter train separation distances as a result from the shorter sections. Any effects of the track discretisation on the underlying rescheduling solutions is non-apparent. The results from the junction case study show some effects of the track discretisation on conflict detection and resolution. Though by far the most benefit in objective value between solutions is due to the shorter train separation resulting from the shorter sections, in some delay scenarios different rescheduling decisions proved to be better for different discretisations. Mostly, the different decisions concern a limited number of route assignments, but occasionally also a train ordering. These are enabled by the short separation in general, enforced by the new separation constraints at switches.

The reported results indicate maximum section lengths of 400 or 200 m as possible thresholds in terms of the balance between solution quality and complexity. Focusing on the rescheduling decisions, the 800-m discretisation already performs well, providing stable and reliable solutions, particularly for the corridor case study. In general, the appropriate discretisation threshold strongly

depends on the case study and its track layout. Hence, a next step is to look into case study characteristics such as track layout, traffic density and delays to identify possible predictors for the effects of track discretisation on conflict detection and resolution.

On the way to practical implementation of conflict detection and resolution models for next-generation signalling systems, further research is needed. For example, into the type of track discretisation; whether uniform sections lengths or 'location-specific' lengths would result in a better balance in complexity and solution quality. Furthermore, it would be interesting to assess the impact of track discretisation on other conflict detection and resolution algorithm, both within and beyond MILP-based approaches. Specially, it is recommended to look into alternative methods for the implementation of the problem, especially with an eye on the real-time nature of the problem.

Declaration of competing interest

The authors declare the following financial interests/personal relationships which may be considered as potential competing interests: Co-author is editor in chief at Journal of Rail Transport Planning & Management - R.M.P. Goverde. Co-author is associate editor at Journal of Rail Transport Planning & Management - J. Rodriguez.

Acknowledgments

This research has received funding from the Shift2Rail Joint Undertaking (JU) under grant agreement No. 101015416 (PERFORMINGRAIL). The JU receives support from the European Union's Horizon 2020 research and innovation programme and the Shift2Rail JU members other than the Union.

Appendix A. MILP formulation for distance-to-go conflict detection and resolution

From Versluis et al. (2024a).

A.1. Sets, parameters and variables

The sets, parameters and variables of the model are listed in Table A.1.

A.2. Model

The fixed-block distance-to-go version of RECIFE-MILP is given by Equations ((A.1)) to ((A.17)).

$$\text{minimise} \quad \sum_{t\in T}\left(w_t(z_t+\sum_{s\in S_t} z_{t,s}) + w\sum_{\substack{r\in R_t:\\ l\in \mathrm{P}^r}} v^{\mathrm{m}}_{t,r,l}\right) \tag{A.1}$$

$$\text{s.t.} \quad o_{t,r,l} \geq init_t\, x_{t,r} \qquad \forall t\in T,\ r\in R_t,\ l\in L^r, \tag{A.2}$$

$$o_{t,r,l} \leq M\, x_{t,r} \qquad \forall t\in T,\ r\in R_t,\ l\in L^r, \tag{A.3}$$

$$\sum_{r\in R_t} x_{t,r} = 1 \qquad \forall t\in T, \tag{A.4}$$

$$v^{\mathrm{m}}_{t,r,l} + v^{\mathrm{s}}_{t,r,l} = x_{t,r} \qquad \forall t\in T,\ r\in R_t,\ l\in \mathrm{P}^r, \tag{A.5}$$

$$o_{t,r,\sigma_{r,l}} = o_{t,r,l} + o^{+}_{t,r,l} + rt_{t,r,l}\, x_{t,r} + \Delta rt_{t,r,l} v^{\mathrm{s}}_{t,r,\rho_{r,l}} \qquad \forall t\in T,\ r\in R_t,\ l\in L^r, \tag{A.6}$$

$$o^{+}_{t,r,l} \geq \sum_{\substack{s\in S_t:\\ l\in S_{t,s}\cap L^r}} dw_{t,s}\, x_{t,r} \qquad \forall t\in T,\ r\in R_t,\ l\in \bigcup_{s\in S_t} L_{t,s}, \tag{A.7}$$

$$o_{t,r,\sigma_{r,l}} \geq \sum_{\substack{s\in S_t:\\ l\in L_{t,s}\cap L^r}} d_{t,s}\, x_{t,r} \qquad \forall t\in T,\ r\in R_t,\ l\in \bigcup_{s\in S_t} L_{t,s}, \tag{A.8}$$

$$z_{t,s} \geq \sum_{r\in R_t}\sum_{l\in L^r\cap L_{t,s}} \left(o_{t,r,l} + rt_{r,t,l} x_{t,r} + \Delta rt_{t,r,l} v^{\mathrm{s}}_{t,r,\rho_{r,l}}\right) - a_{t,s} \qquad \forall t\in T, s\in S_t, \tag{A.9}$$

$$z_t \geq \sum_{r\in R_t} o_{t,r,l_\infty} - sched_t \qquad \forall t\in T, \tag{A.10}$$

$$b^{\mathrm{s}}_{t,l} \leq \sum_{\substack{r\in R_t:\\ l\in L^r}} \left(o_{t,r,ref^{\mathrm{s}}_{t,r,l}} + \left(lag^{\mathrm{s}}_{t,r,l} - for_{r,l}\right) x_{t,r}\right) \qquad \forall t\in T,\ l\in L_t : s_l = 0 \vee \nexists r\in R_t : s_{\pi_{r,l}} = 1, \tag{A.11}$$

Table A.1
Sets, parameters and variables for the MILP model formulation.

Sets	
T	Ordered set of trains
R	Set of routes
$R_t \subset R$	Set of routes available to train $t \in T$
L	Set of locations
$L_t \subset L$	Set of locations which can be used by train $t \in T$
$L^r \subset L$	Set of locations along route $r \in R$
$OL_{t,r,l} \subset L^r$	Set of locations along route $r \in R_t$ such that if train $t \in T$ starts occupying it, the train has not yet cleared location $l \in L^r$, $l \notin OL_{t,r,l}$
S	Set of stations
$S_t \subset S$	Set of stations where train $t \in T$ has a scheduled stop
$L_{t,s} \subset L_t$	Set of locations that can be used by train $t \in T$ for stopping at station $s \in S_t$
$\hat{L}_{t,t',l} \subset L$	Set of locations $l' \in L_t \cap L_{t'}$ which may be used by trains $t, t' \in T$ such that if t precedes t' on l, then t precedes t' on l'
$\mathrm{P} \subset L$	Set of speed assignment locations
$\mathrm{P}^r \subset \mathrm{P}$	Set of speed assignment locations along route $r \in R$
Parameters	
$\pi_{r,l}, \sigma_{r,l} \in L^r$	Preceding location and succeeding location of location $l \in L^r$ along route $r \in R$
$\rho_{r,l} \in \mathrm{P}^r$	Speed assignment location associated with location $l \in L^r$ along route $r \in R$
$s_l \in \{0,1\}$	$= 1$ if location $l \in L$ lies in a switch area
$l_\infty \in L$	Dummy location considered as destination for all trains
$init_t \in \mathbb{R}_+$	Earliest time at which train $t \in T$ can be operated
$sched_t \in \mathbb{R}_+$	Scheduled arrival time of train $t \in T$ at dummy destination location $l_\infty \in L$
$dw_{t,s} \in \mathbb{R}_+$	Minimum dwell time for train $t \in T$ at station $s \in S_t$
$a_{t,s}, d_{t,s} \in \mathbb{R}_+$	Scheduled arrival/departure time for train $t \in T$ at station $s \in S_t$
$for_{r,l} \in \mathbb{R}_+$	Formation time, i.e., setup and reaction time, of location $l \in L^r$ along route $r \in R$
$rel_{r,l} \in \mathbb{R}_+$	Release time of location $l \in L^r$ along route $r \in R$
$rt_{t,r,l} \in \mathbb{R}_+$	Minimum running time for train $t \in T$ from location $l \in L_t$ to $\sigma_{r,l}$ along route $r \in R_t$
$\Delta rt_{t,r,l} \in \mathbb{R}_+$	Additional running time for train $t \in T$ from location $l \in L_t$ to $\sigma_{r,l}$ along route $r \in R_t$ in case of scheduled speed profile
$ct_{t,r,l} \in \mathbb{R}_+$	Minimum clearing time for train $t \in T$ of location $l \in L_t$ along route $r \in R_t$
$\Delta ct_{t,r,l} \in \mathbb{R}_+$	Additional clearing time for train $t \in T$ of location $l \in L_t$ along route $r \in R_t$ in case of scheduled speed profile
$ref^{\mathrm{s}}_{t,r,l} \in L^r$	Reference brake location for location $l \in L^r$ along route $r \in R_t$ for train $t \in T$ approaching according to scheduled speed profile
$ref^{\mathrm{m}}_{t,r,l} \in L^r$	Reference brake location for location $l \in L^r$ along route $r \in R_t$ for train $t \in T$ approaching according to maximum speed profile
$lag^{\mathrm{s}}_{t,r,l} \in \mathbb{R}_+$	Time by which blocking of location $l \in L^r$ by train $t \in T$ running according to scheduled speed profile along route $r \in R_t$ can be postponed after passing $ref^s_{t,r,l}$
$lag^{\mathrm{m}}_{t,r,l} \in \mathbb{R}_+$	Time by which blocking of location $l \in L^r$ by train $t \in T$ running according to maximum speed profile along route $r \in R_t$ can be postponed after passing $ref^m_{t,r,l}$
$M \in \mathbb{R}_+$	A large constant
$w, w_t \in \mathbb{R}_+$	Maximum speed profile penalty and train priority weights for objective function
Variables	
$y_{t,t',l} \in \{0,1\}$	$= 1$ if train $t \in T$ blocks location $l \in L_t \cap L_{t'}$ before train $t' \in T$
$x_{t,r} \in \{0,1\}$	$= 1$ if train $t \in T$ uses route $r \in R_t$
$v^{\mathrm{s}}_{t,r,l} \in \{0,1\}$	$= 1$ if train $t \in T$ passes speed assignment location $l \in \mathrm{P}^r$ along route $r \in R_t$ according to scheduled speed profile
$v^{\mathrm{m}}_{t,r,l} \in \{0,1\}$	$= 1$ if train $t \in T$ passes speed assignment location $l \in \mathrm{P}^r$ along route $r \in R_t$ according to maximum speed profile
$o_{t,r,l} \in \mathbb{R}_+$	Occupation starting time of train $t \in T$ on location $l \in L^r$ along route $r \in R_t$
$o^+_{t,r,l} \in \mathbb{R}_+$	Extended occupation time of train $t \in T$ between locations $l \in L^r$ and $\sigma_{r,l} \in L^r$ along route $r \in R_t$
$b^{\mathrm{s}}_{t,l}, b^{\mathrm{e}}_{t,l} \in \mathbb{R}_+$	Time at which train $t \in T$ starts/ends blocking location $l \in L_t$
$z_t \in \mathbb{R}_+$	Delay suffered by train $t \in T$ when exiting the infrastructure and/or arriving at destination
$z_{t,s} \in \mathbb{R}_+$	Delay suffered by train $t \in T$ when stopping at station $s \in S_t$

$$b^{\mathrm{s}}_{t,l} \le \sum_{\substack{r \in R_t: \\ l \in L^r}} \left(o_{t,r,ref^{\mathrm{m}}_{t,r,l}} + \left(lag^{\mathrm{m}}_{t,r,l} - for_{r,l} \right) x_{t,r} + M\, v^{\mathrm{s}}_{t,r,\rho_{r,ref^s_{t,r,l}}} \right)$$

$$\forall t \in T,\ l \in L_t : s_l = 0 \vee \nexists r \in R_t : s_{\pi_{r,l}} = 1, \tag{A.12}$$

$$b^{\mathrm{s}}_{t,l} \le \sum_{\substack{r \in R_t: \\ l \in L^r}} \left(o_{t,r,ref^{\mathrm{s}}_{t,r,\pi_{r,l}}} + \left(lag^{\mathrm{s}}_{t,r,\pi_{r,l}} - for_{r,\pi_{r,l}} \right) x_{t,r} \right.$$

$$\forall t \in T,\ l \in L_t : s_l = 1 \wedge \exists r \in R_t : s_{\pi_{r,l}} = 1, \tag{A.13}$$

$$b^{\mathrm{s}}_{t,l} \le \sum_{\substack{r \in R_t: \\ l \in L^r}} \left(o_{t,r,ref^{\mathrm{m}}_{t,r,\pi_{r,l}}} + \left(lag^{\mathrm{m}}_{t,r,\pi_{r,l}} - for_{r,\pi_{r,l}} \right) x_{t,r} + M\, v^{\mathrm{s}}_{t,r,\rho_{r,ref^s_{t,r,\pi_{r,l}}}} \right)$$

$$\forall t \in T,\ l \in L_t : s_l = 1 \wedge \exists r \in R_t : s_{\pi_{r,l}} = 1, \tag{A.14}$$

$$b^{e}_{t,l} = \sum_{\substack{r \in R_t : \\ l \in L^r}} \left(o_{t,r,\sigma_{r,l}} + \left(ct_{t,r,l} + rel_{r,l} \right) x_{t,r} + \Delta ct_{t,r,l} v^{s}_{t,r,\rho_{r,l}} + \sum_{\substack{l' \in L^r : \\ l' \in OL_{t,r,l}}} o^{+}_{t,r,l'} \right)$$

$$\forall t \in T,\ l \in L_t, \tag{A.15}$$

$$b^{e}_{t,l} - M\,(1 - y_{t,t',\hat{l}}) \le b^{s}_{t',l} \qquad \forall t, t' \in T, t \prec t',\ l, \hat{l} \in L_t \cap L_{t'} : l \in \hat{L}_{t,t',\hat{l}}, \tag{A.16}$$

$$b^{e}_{t',l} - M\,y_{t,t',\hat{l}} \le b^{s}_{t,l} \qquad \forall t, t' \in T, t \prec t',\ l, \hat{l} \in L_t \cap L_{t'} : l \in \hat{L}_{t,t',\hat{l}}. \tag{A.17}$$

References

Benders, J.F., 1962. Partitioning procedures for solving mixed-variables programming problems. Numer. Math. 4, 238–252.

Bettinelli, A., Santini, A., Vigo, D., 2017. A real-time conflict solution algorithm for the train rescheduling problem. Transp. Res. Part B: Methodol. 106, 237–265.

Cacchiani, V., Huisman, D., Kidd, M., Kroon, L., Toth, P., Veelenturf, L., Wagenaar, J., 2014. An overview of recovery models and algorithms for real-time railway rescheduling. Transp. Res. Part B: Methodol. 63, 15–37.

Caimi, G., Fuchsberger, M., Laumanns, M., Lüthi, M., 2012. A model predictive control approach for discrete-time rescheduling in complex central railway station areas. Comput. Oper. Res. 39, 2578–2593.

Corman, F., D'Ariano, A., Pacciarelli, D., Pranzo, M., 2009. Evaluation of green wave policy in real-time railway traffic management. Transp. Res. Part C: Emerg. Technol. 17 (6), 607–616.

Cuppi, F., Vignali, V., Lantieri, C., Rapagnà, L., Dimola, N., Galasso, T., 2021. High density European rail traffic management system (HD-ERTMS) for urban railway nodes: The case study of Rome. J. Rail Transp. Plan. Manag. 17, 100232.

D'Ariano, A., 2008. Improving Real-Time Train Dispatching: Models, Algorithms and Applications (Ph.D. thesis). Delft University of Technology, The Netherlands.

EEIG ERTMS Users Group, 2024. ERTMS/ETCS hybrid train detection: Principles.

European Rail Supply Industry Association, 2022. ERTMS. https://www.ertms.net/.

European Railway Agency, 2020. Introduction to ETCS braking curves.

Furness, N., Van Houten, H., Arenas, L., Bartholomeus, M., 2017. ERTMS level 3: the game-changer. IRSE News 232, 2–9.

Hansen, I.A., Pachl, J. (Eds.), 2014. Railway Timetabling & Operations: Analysis, Modelling, Optimisation, Simulation, Performance Evaluation. Eurail Press, Hamburg, Germany.

Jansen, J.M., 2019. ERTMS/ETCS Hybrid Level 3: A Simulation-Based Impact Assessment for the Dutch Railway Network (Master's thesis). Delft University of Technology.

Janssens, M.L., 2022. Multi Machine Approaches for Conflict Resolution under Moving Block Signalling (Master's thesis). Delft University of Technology, The Netherlands.

Knutsen, D., Olsson, N.O.E., Fu, J., 2024. Capacity evaluation of ERTMS/ETCS hybrid level 3 using simulation methods. J. Rail Transp. Plan. Manag. 30, 100444.

Lamorgese, L., Mannino, C., 2015. An exact decomposition approach for the real-time train dispatching problem. Oper. Res. 63 (1), 48–64.

Lippes, S.J.H., 2024. Distributed Rail Traffic Management under Moving-Block Signalling (Master's thesis). Delft University of Technology, The Netherlands.

Liu, F., Xun, J., Liu, R., Yin, J., Dong, H., 2021. A real-time rescheduling approach by using loop iteration for high-speed railway traffic. IEEE Intell. Transp. Syst. Mag. 15 (1), 318–332.

Luan, X., Wang, Y., De Schutter, B., Meng, L., Lodewijks, G., Corman, F., 2018. Integration of real-time traffic management and train control for rail networks - Part 1: Optimization problems and solution approaches. Transp. Res. Part B: Methodol. 115, 41–71.

Lusby, R.M., Larsen, J., Ehrgott, M., Ryan, D.M., 2013. A set packing inspired method for real-time junction train routing. Comput. Oper. Res. 40, 713–724.

Marlière, G., Sobieraj Richard, S., Pellegrini, P., Rodriguez, J., 2023. A conditional time-intervals formulation of the real-time railway traffic management problem. Control Eng. Pract. 54 (2), 187–194.

Mazzarello, M., Ottiviani, E., 2007. A traffic management system for real-time traffic optimisation in railways. Transp. Res. Part B: Methodol. 41 (2), 246–274.

Pellegrini, P., Marlière, G., Pesenti, R., Rodriguez, J., 2015. RECIFE-MILP: An effective MILP-based heuristic for the real-time railway traffic management problem. IEEE Trans. Intell. Transp. Syst. 16 (5), 2609–2619.

Pellegrini, P., Marlière, G., Rodriguez, J., 2014. Optimal train routing and scheduling for managing traffic perturbations in complex junctions. Transp. Res. Part B: Methodol. 59, 58–80.

PERFORMINGRAIL, 2022. Deliverable D4.1: Real-time traffic rescheduling algorithms for perturbation management and hazard prevention in moving-block operations.

Pochet, J., Baro, S., Sandou, G., 2016. Supervision and rescheduling of a mixed CBTC traffic on a suburban railway line. In: 2016 IEEE International Conference on Intelligent Rail Transportation. ICIRT.

Ranjbar, V., Olsson, N.O.E., Sipilä, H., 2022. Impact of signalling system on capacity – comparing legacy ATC, ETCS level 2 and ETCS hybrid level 3 systems. J. Rail Transp. Plan. Manag. 23, 100322.

Reynolds, E., Ehrgott, M., Maher, S.J., Patman, A., Wang, J.Y.T., 2020. A multicommodity flow model for rerouting and retiming trains in real-time to reduce reactionary delay in complex station areas. Optim. Online.

Rodriguez, J., 2007. A constraint programming model for real-time train scheduling at junctions. Transp. Res. Part B: Methodol. 41 (2), 231–245.

Shift2Rail, 2023. https://projects.shift2rail.org/s2r_ip2_n.aspx?p=S2R_PERFORMINGRAIL,

Törnquist, J., Persson, J., 2007. N-tracked railway traffic re-scheduling during disturbances. Transp. Res. Part B: Methodol. 41 (3), 342–362.

Vergroesen, R., 2020. ERTMS/ETCS Hybrid Level 3 and ATO: A Simulation-Based Capacity Impact Study for the Dutch Railway Network (Master's thesis). Delft University of Technology.

Versluis, N.D., Pellegrini, P., Quaglietta, E., Goverde, R.M.P., Rodriguez, J., 2024a. Conflict detection and resolution for distance-to-go railway signalling. Preprint available at SSRN: https://ssrn.com/abstract=4760723.

Versluis, N.D., Quaglietta, E., Goverde, R.M.P., Pellegrini, P., Rodriguez, J., 2024b. Real-time railway traffic management under moving-block signalling: A literature review and research agenda. Transp. Res. Part C: Emerg. Technol. 158, 104438.

Xu, P., Corman, F., Peng, Q., Luan, X., 2017. A train rescheduling model integrating speed management during disruptions of high-speed traffic under a quasi-moving block system. Transp. Res. Part B: Methodol. 104, 638–666.

Xu, P., Zhang, D., Guo, J., Liu, D., Peng, H., 2021. Integrated train rescheduling and rerouting during multidisturbances under a quasi-moving block system. J. Adv. Transp. 2021, 6652531.

Yi, X., Marlière, G., Pellegrini, P., Rodriguez, J., Pesenti, R., 2023. Coordinated train rerouting and rescheduling in large infrastructures. Transp. Res. Procedia 72, 319–326.